

A COMPARISON OF TRACHEAL MORPHOLOGY AND ELASTIN ABUNDANCE IN
BOTTLENOSE DOLPHIN (CETACEA: *Tursiops truncatus*) AND WHITE-TAILED DEER
(ARTIODACTYLA: *Odocoileus virginianus*)

A Thesis

by

ANDREW A. SCERBO

BS, Texas A&M University-Corpus Christi, 2010

Submitted in Partial Fulfillment of the Requirements for the Degree of

MASTER of SCIENCE

in

BIOLOGY

Texas A&M University-Corpus Christi
Corpus Christi, Texas

May 2018

© Andrew A. Scerbo

All Rights Reserved

May 2018

A COMPARISON OF TRACHEAL MORPHOLOGY AND ELASTIN ABUNDANCE IN
BOTTLENOSE DOLPHIN (CETACEA: *Tursiops truncatus*) AND WHITE-TAILED DEER
(ARTIODACTYLA: *Odocoileus virginianus*)

A Thesis

by

ANDREW A. SCERBO

This thesis meets the standards for scope and quality of
Texas A&M University-Corpus Christi and is hereby approved

Riccardo Mozzachiodi, PhD
Co-Chair

David Moury, PhD
Co-Chair

Kim Withers, PhD
Committee Member

Ed Proffitt, PhD
Chair, Department of Life Sciences

May 2018

ABSTRACT

Odontocete species exhibit diving strategies to exploit various resources in marine waters. While the phenomenon of lung collapse has been studied, the morphology and fine structure of the respiratory conducting regions are largely unexplored. A comparison of elastin abundance and tracheal morphology between marine and terrestrial mammals is needed to explore this question. The aim of this study was to compare and contrast the tracheal regions between two species of mammal that experience a wide differential in pressure gradients. Tracheae from Atlantic bottlenose dolphins (*Tursiops truncatus*) and white-tailed deer (*Odocoileus virginianus*) were collected and examined using gross morphology and light microscopy. This study showed that differences in tracheal dimensions, architecture, cartilaginous ring structure and elastin abundance were the result of divergent adaptations to lifestyles exploiting very different environments. There was a significant difference in elastin coverage (percent) with more elastin in *Tursiops truncatus* than in *Odocoileus virginianus*. The respiratory system of terrestrial *Odocoileus virginianus* evolved for flexibility and increased range of motion; whereas, the odontocete airway became more compact, rigid and reinforced to contend with the increased pressures associated with an aquatic environment.

ACKNOWLEDGMENTS

First, I would like to thank the original members of my committee as a group, – Dr. David Moury, Dr. Andreas Fahlman and Dr. Riccardo Mozzachiodi for their participation in this project; and to additionally thank Dr. Kim Withers for agreeing to participate long after this project was underway. You have all stood by me for the long run and my gratitude is nearly as infinite as your patience. Dr. Mozzachiodi, your ability to make the most of every moment of a conversation is truly inspiring. Dr. Fahlman, for your perspectives and analytical skills that help to obfuscate the obvious; your experimental design skills are second to none. And Dr. Moury... your mentorship is but the tip of the iceberg. You helped show me how to be a better scientist and a person; there has been no more influential mentor in my life. Thank you for inducting me into the world of “mad science”.

Thanks also to one of my former committee members, Dr. David McKee. Your generosity was very influential in many aspects. When I desperately needed your assistance in this project, you came through for me.

I would also like to thank several other impactful professors from my time here in Corpus Christi. It is with great regret that both Dr. Bart Cook and Dr. Graham Hickman passed away during my tenure at Texas A&M University-Corpus Christi. Both were highly influential instructors that showed masterful guidance with students and their passion for science.

I must also thank the Texas Marine Mammal Stranding Network for igniting my passion for marine mammals in a very tangible way. The leadership and dedication of TMMSN Regional Coordinator, Lea Walker, has been a whole other curriculum in and of itself. Also, thanks to my colleague and fellow TMMSN zealot, Elani Morgan-Eckert; your unparalleled kindness and

tolerance are as inspiring as your passion. Many others from TMMSN have inspired, taught and made a definite impact upon me; Garrett Eccleston, Gary Walker, Ken Brown, Kelsey Tatsch, Sunnie Brenneman, Theresa Mitchell, David Williams, Trip Thomas, Stump Levitt, Heidi & Chris Whitehead, Errol Ronje and many more. I can't list all of your individual contributions, but I will certainly remember them.

I could not hope to complete this section without thanking my incredibly supportive family. As my bedrock, you have stood by me through so many initiatives and your encouragement has never waned; even when I gave you plenty of reason. You allowed me to “trip the light fantastic” during this academic venture and never gave me reason to question this path. My benign insanity was cultivated and encouraged by all of you. To my friend, Steven Lowe...you are part of my family and I am grateful for over 25 years of friendship and camaraderie; you've always been one to tell me the truth, regardless of circumstances. Martin Donley, whose friendship and fellowship helped keep me sane during the impossibly long hours in labs and classes.

I also need to thank a myriad of other individuals who have helped me in a myriad of means. Geri Fernandez and Ken Brown never let me down with any request. Thanks to the OBX Marine Mammal Stranding Network for the majority of the samples used in this study, NOAA/NMFS for the permits required, Dr. Lee Smee for loaning me a few chemicals during extremely sensitive time-frames and Dr. Colby Moore-Reilly, for her collaboration efforts and suggestions. Thanks also to Brooke Stanford, Phil Jose, Galyen Nuckols and Dale Cochran for many favors above and beyond the call of duty as lab coordinators.

And, finally, Dr. Kim Withers, who was added late to this endeavor, but who never failed to offer excellent mentorship from personal and academic standpoints. You may be the last to offer assistance on this venture, but you are certainly not the least.

TABLE OF CONTENTS

CONTENTS	PAGE
ABSTRACT.....	v
ACKNOWLEDGMENTS	vi
TABLE OF CONTENTS.....	viii
LIST OF FIGURES	x
LIST OF TABLES	xi
INTRODUCTION	1
Structure of the Mammalian Trachea	1
Objectives	7
METHODS	9
Data Collection.....	10
Data Analysis	16
RESULTS	18
General tracheal characteristics.....	18
Fine Morphology of the Trachea.....	20
Elastin Coverage and Distribution	24
Elastin content evaluation	26
DISCUSSION.....	28
Gross Morphology.....	28

Fine Structure	30
Future Directions	32
LITERATURE CITED	34
APPENDIX A.....	39
APPENDIX B	43
APPENDIX C	44
APPENDIX D.....	54
APPENDIX E	55
APPENDIX F.....	56
APPENDIX G.....	61

LIST OF FIGURES

FIGURES	PAGE
Figure 1. Illustration of head and respiratory system of an odontocete.....	3
Figure 2. Morphology of an odontocete trachea.....	4
Figure 3. Defining dolphin tracheal regions and subregions.....	11
Figure 4. Example of subsection regionalization.....	14
Figure 5. Example of adjusting photomicrographs.....	15
Figure 6. Determining proportional data value from a thresholded image.....	16
Figure 7. Tracheal differences in gross anatomy.....	19
Figure 8. Examples of subregional tissue sections in the two species.....	21
Figure 9. Fine structure tracheal differences between species.....	23
Figure 10. Epithelium of <i>O. virginianus</i> (Ov) and the <i>T. truncatus</i> (Tt).....	24
Figure 11. Comparison of Distal/dorsal (Dd) tracheal tissues.....	25
Figure 12. Overall means of elastin coverage with standard error for each species.....	27

LIST OF TABLES

TABLES	PAGE
Table 1. Mean values for elastin coverage (in %)	26

LIST OF APPENDICES

APPENDIX		PAGE
APPENDIX A	National Marine Fisheries Service Permit.....	40
APPENDIX B	Species specimen data and tracheal dimensions.....	44
TABLE B1	Specimen data and tracheal dimensions.....	44
TABLE B2	Specimen tracheal means and standard error.....	44
APPENDIX C	Specimen regional and subregional elastin data.....	45
APPENDIX D	Normality test for species population data.....	55
APPENDIX E	Intraspecies regional and subregional variation.....	56
TABLE E1	ANOVA results for region and subregion variation.....	56
TABLE E2	Species regional and subregional means.....	56
APPENDIX F	Circumferential examination of dolphin tracheal rings..	57
APPENDIX G	Species tracheae with photomicrographs.....	62
FIGURE G1	Dolphin trachea with regional sections	62
FIGURE G2	Deer trachea with regional section.....	63

INTRODUCTION

Unlike terrestrial mammals, marine mammal airways must remain functional under a wide variety of pressure conditions (Kooyman 1989). Terrestrial mammals have reliable access to air and respire via perpetual alternation of inhalations and exhalations. Cetacean respiration is an intermittent mechanism in that each inhalation and subsequent exhalation are separated by a period of apnea (Berta et al. 2005); in fact, they spend more time holding their breath than actively exchanging air. The varying pressure gradient inherent to an aquatic lifestyle (an increase of 1.0 atmospheres of pressure every 10 m of depth) means that adaptations in respiratory structure are necessary for marine mammal survival. Comparing tracheal structures of an aquatic marine mammal species and a terrestrial relative with recent common ancestry could illustrate how these species adapted to different environments and different respiratory behaviors. The goal of the research is to determine if there are obvious adaptations in the trachea related to the lifestyle differences of Atlantic bottlenose dolphin (*Tursiops truncatus*) and white-tailed deer (*Odocoileus virginianus*).

Many studies have examined the lungs of marine mammals, but the conducting portion of the respiratory system, the trachea and associated structures, has been largely ignored. Tracheal studies of marine mammals have mostly focused upon pulmonary systems and forced diving experiments but the fine structure of the marine mammalian trachea is poorly described. Most studies have examined mechanical pliability, but rarely focus upon tracheal structures (e.g., cartilaginous rings) and associated tissues (Fanning and Harrison 1974, Snyder 1983, Cozzi et al. 2005, Bostrom et al. 2008, Bagnoli et al. 2011, Davenport et al. 2013, Moore et al. 2014).

Structure of the Mammalian Trachea

Marine mammal respiratory systems have evolved in response to their movement from the land to the sea (Boyden and Gemeroy 1950; O'Leary and Geisler 1999). These adaptations are constrained by their terrestrial origin (Davenport et al. 2013). The existing terrestrial architecture (e.g., lungs, diaphragm,

trachea) had to be adapted for breath-hold and dive behaviors. The airway of modern odontocetes begins at the dorsally located blowhole (Fig. 1) and continues downward as a nasal passage anterior to the cranium. The external nares have migrated from the anterior terminus to the top of the head. The odontocete airway has also become completely separated from the pharynx and esophagus, unlike terrestrial mammals. Cetaceans have shorter necks than their terrestrial relatives and shorter distances to the lungs have resulted in shortening of the tracheae (Fanning 1977; Romer and Parsons 1977; Davenport et al. 2013). The combination of the neck shortening and the migration of the airway to the apex of the head brought the respiratory tract to a vertical alignment posterior to the oral cavity in an orthogonal orientation, resulting in the esophagus bifurcating around the laryngeal junction (“goose beak”); the esophagus reunites posterior to the respiratory passageway continuing toward the stomach on the dorsal side of the trachea.

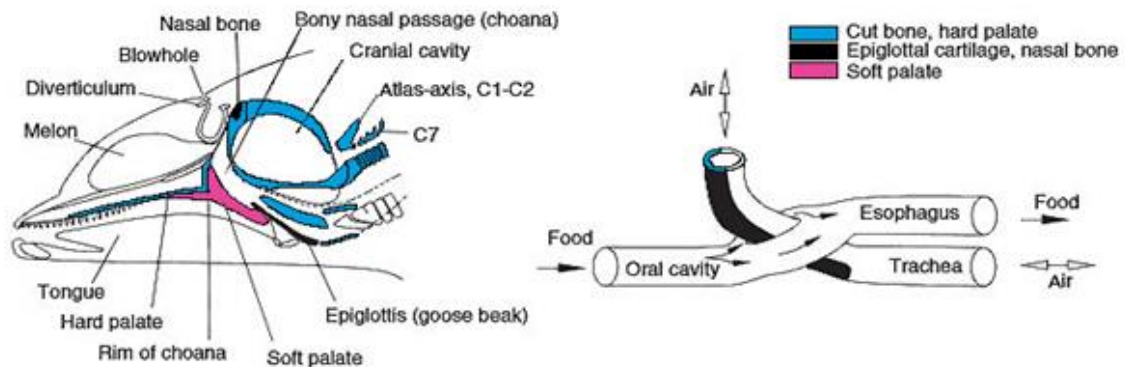


Figure 1. Illustration of head and respiratory system of an odontocete. Left, illustration showing the respiratory passage from blowhole to trachea; right, the trachea and its relationship with the bifurcating esophagus. Modified from Rommel et al. (2009).

The epiglottis and corniculate cartilages forming the “goose beak” junction connect the vertical nasal passage anteriorly to the trachea (immediately posterior to the cricoid cartilage) forming an obtuse angle (Reidenberg and Laitman 1987; Smith et al. 1999). The “C”-shaped incomplete cartilaginous rings

of terrestrial mammalian tracheae have evolved into a series of completely circular “O”-shaped structures in most odontocetes. The stiffened airways counteract increased water pressure (Thiberville et al. 2007). The tracheal rings have become wide and thick compared to the narrow, thin tracheal rings of their terrestrial ancestors and adjacent rings have grown closer together (Tarasoff and Kooyman 1973).

Marine mammal tracheae are wide and asymmetrical in odontocetes. Approximately one-third of the distance posterior from the cranially located cricoid cartilage, a right tracheal bronchus bifurcates from the main body of the trachea and extends to the right lung (Fanning and Harrison 1974, Bagnoli et al. 2011). At the caudal end of the trachea, the main bifurcation (carina) separates into uneven bronchi. The left bronchus is considerably larger than the right bronchus (Fig. 2) although the two right bronchi combined have a larger overall luminal volume (Tsang et al. 2002). The lumen of the main body of the trachea is larger in diameter in odontocetes than comparable terrestrial mammals (Cozzi et al. 2005) which may increase the risk of collapse while diving.

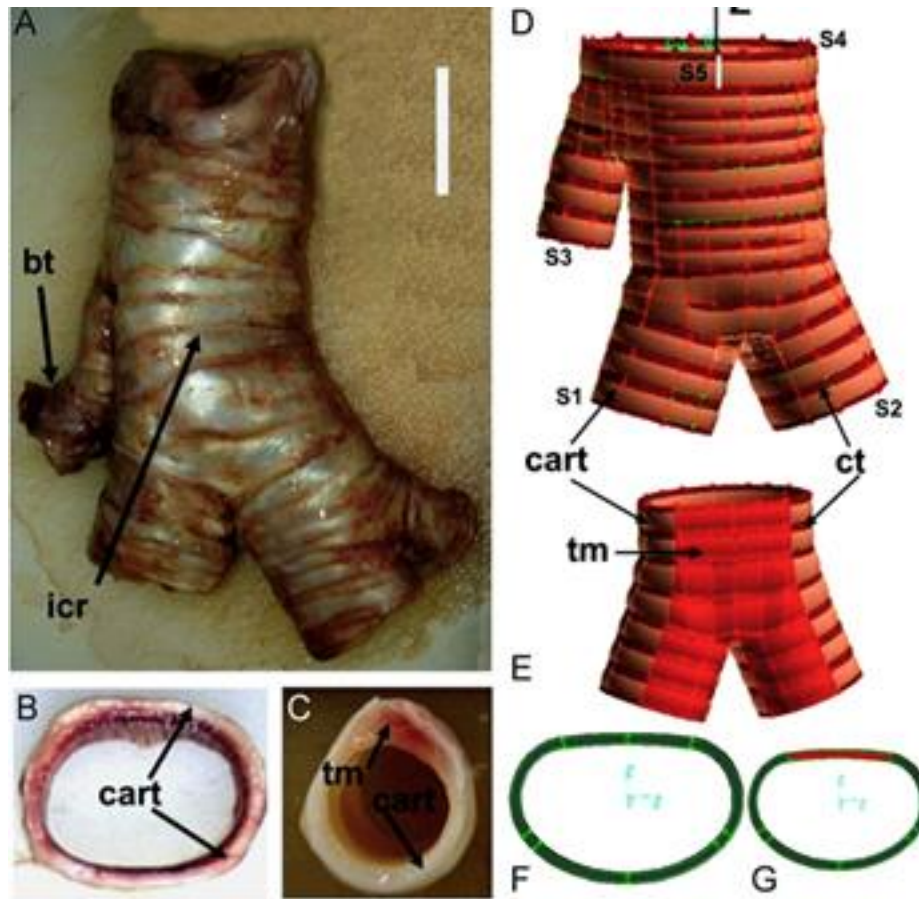


Figure 2. Morphology of an odontocete trachea. A, B, C, D, and F illustrate the bronchus trachealis (bt), irregular cartilaginous ring (icr), cartilaginous rings (cart), tracheal mucosa (tm) and connective tissue (ct) with the trachea of a terrestrial mammal (E and G). From Bagnoli et al. (2011).

In general, the tracheae of terrestrial mammals exhibit an ordered pseudostratified epithelium and consistently incomplete “C-shaped” cartilaginous rings, the dorsally located free portions of which are connected by a flexible trachealis muscle that extends the full length of the trachea. Odontocete tracheae do not exhibit these properties (Fanning and Harrison 1974). The epithelia of several odontocete species are lined by transitional epithelium (Fanning and Harrison 1974, Cozzi et al. 1994). Epithelia of this type indicate regions of tissue expansion. Expanding tissues in conjunction with thin elastic connective tissues interspersed between the cartilaginous tracheal rings may indicate a stress point where tissue must rapidly

rearrange itself into normal conformation after pressure is relieved (Romer and Parsons 1977, Starcher 1986).

Integration of Structure, Function, and Life History

While there are subtle variations among species, many of the differences may be attributed to different diving strategies. Shallow divers, such as sea otters (*Enhydra lutris*), have calcified tracheal rings to keep their airways open under minor pressures (Scholander 1940). However because *Tursiops truncatus* dives deeper than sea otters (even though not as deep as some other odontocetes), calcification of the tracheal rings would likely not be enough to keep the airway open (Scholander 1940). Forced diving experiments in hyperbaric chambers performed in the late 1960's illustrated that some collapse of the trachea was unavoidable at certain depths (Kooyman et al. 1970). Kooyman and Ponganis (1998) postulated that a more compliant trachea may increase the depths at which alveolar collapse reaches complete atelectasis (i.e., progressive alveolar collapse), yet the resistance of the trachea to external pressures is influenced by whether or not marine mammals begin their dive with a lung full of air or after exhalation (Piscitelli et al. 2013). While some odontocetes exhale just before diving, some do not (Scholander 1940, Kooyman et al. 1970, Ponganis 2011). *Tursiops truncatus* uses both behaviors, but with its abundant hemoglobin and myoglobin, a full air supply in the lungs is not necessary if its surface interval is long enough to replenish hemoglobin and myoglobin oxygen stores. Because of its oxygen "storage" capacity, *Tursiops truncatus* has a smaller lung capacity (by volume) for their size than terrestrial mammals (Schmidt-Nielson 1984, Kooyman 1985).

Although marine mammals encounter many problems while contending with increasing depth and diving durations (Kooyman 1989), a primary concern is the likelihood of developing decompression sickness. Nitrogen gas is in such close proximity to the respiratory surfaces of the alveoli that increasing pressures at depth can force the inert gas into the bloodstream. As the organism approaches the surface (and pressure decreases), nitrogen gas cannot diffuse out of the body quickly and can collect in the

bloodstream and within joints causing tissue damage and blocking blood vessels. Complete or partial collapse of the lung (atelectasis) restricts the exchange of gases between the trapped air and the blood, reduces uptake of nitrogen gases, and increases the likelihood of decompression sickness (Ridgway and Howard 1979; Falke et al. 1985; Fahlman et al. 2006). Scholander (1940) postulated that marine mammal lungs collapse during diving, forcing the contained gases to move out of the lungs and into the conducting region of the tracheobronchial tree. Using a simplistic “balloon and pipe” model, he demonstrated that different portions of the marine mammal respiratory system have varying levels of flexibility (i.e., compliance) and this variation complicates the pressure-volume relationship (Bostrom et al. 2008). If one assumes the air within an enclosed system flows without restrictions, then the internal pressure should be equal throughout the entire respiratory tract. Thus, variation in the compliance of different tissues allows gases to move out of the pliable lungs, into the reinforced conducting regions of the tracheobronchial tree, and back again when pressures are reduced. This mechanism also prevents too much nitrogen gas from entering the bloodstream. Increasing depth will decrease the volume of air within the lungs according to both Boyle’s and Pascal’s laws (Resnick and Halliday 1966; Taylor 1994). Scholander (1940) suggested that marine mammal lungs would collapse at relatively shallow depths (30-50 m) but more recent calculations suggest the depth at which all air in the lungs is transferred into the respiratory conducting apparatus varies by species, and may not occur until a maximum depth of 270 m (Davenport et al. 2013).

At 1000 m, the air chamber of the respiratory tract is reduced by 90% and the larynx has no air available for vocalization (Clarke 2003, Davenport et al. 2013). Yet, vocalization occurs in the vestibular region adjacent to the nasal cavities within most odontocetes where air is available due to the vascular expansion of the tracheal lining (Davenport et al. 2013). The submucosa of the trachea is host to a large vascular plexus that allows the tissue to dilate and reduce the volume of the respiratory tract thus supplying air to the sound producing apparatus in *Tursiops truncatus* (Houser et al. 2004). Upon surfacing, as the ambient pressures reduce, the tissues recoil and the airway becomes patent due to an abundance of an extracellular elastic protein.

Elastin is the component responsible for returning deformed tissue to normal conformation. It is found in blood vessels, epithelium, connective tissue (Song 1994), and many other areas in organisms that stretch, bend, and expand, including the respiratory tract. Elastin flexes more efficiently in response to changing pressure than other tissues. For example, the elasticity of the aorta of whales is significantly greater than that seen in other mammals due to greater amounts of elastin (Gosline and Shadwick 1996). Mammalian tracheae contain substantial amounts of elastin in the mucosa and submucosa. Because the proximal and distal portions of the tracheobronchial tree are more stable because of their attachment to larger structures (larynx, cranially; and lungs caudally), the more exposed and less firmly associated medial portion of the tree collapses more readily. The ellipsoid shape of the trachea combined with the proximity of the ventral surface to the source of external pressure causes the trachea to collapse ventro-dorsally under ambient pressures (Kooyman 1970, Cozzi et al. 2005).

Objectives

In this study, the tracheal structure of white-tailed deer (*Odocoileus virginianus*) was compared and contrasted to Atlantic bottlenose dolphin (*Tursiops truncatus*), two species with a common ancestry (clade Cetartiodactyla; Irwin and Arnason 1994, Price et al. 2005), but very different lifestyles; one aquatic, one terrestrial. *Tursiops truncatus* is an odontocete (toothed whale) from the family Delphinidae (order Cetacea). *Odocoileus virginianus* is an even-toed ungulate (hoofed mammal) from the family Cervidae (order Artiodactyla). At the time of this investigation, no previous study had concentrated on comparing the amount of elastin within marine mammal tracheae. For this study, it was expected that the species exposed to the greatest variation in pressure gradients (*Tursiops truncatus*) would have the most elastin content in its tracheae (both along the long axis and circumferentially) when compared to *Odocoileus virginianus* which is exposed to smaller variations in pressure.

The objectives of this study were to:

1. To compare the gross morphology of the trachea of a terrestrial ungulate species (*Odocoileus virginianus*) and a marine odontocete species (*Tursiops truncatus*).
2. To determine if there are differences in amounts of tracheal elastin between the two species.
 - a. H_0 : There are no significant differences in the abundance of tracheal elastin between *Odocoileus virginianus* and *Tursiops truncatus*
 - b. H_a : There are greater amounts of trachea elastin in one of the species

METHODS

This study was planned to compare the tracheal tree of mammals with different lifestyles (terrestrial and aquatic) at the gross morphological level and then to narrow that focus to a fine structure component, in this case elastin. *Tursiops truncatus* represents an aquatic diver, ~2.5–3 m in length with a mass around 104–240 kg (Ridgway and Fenner 1982, Wells and Scott 1999, Geraci and Lounsbury 2005). *Odocoileus virginianus* represents a non-domesticated ungulate that is comparable in size to *Tursiops truncatus*, ~1.04–2.39 m and 92–183 kg (Saunders 1988).

Collection and preparation of samples

Tracheae from seven Atlantic bottlenose dolphins (*Tursiops truncatus*) were obtained through the OBX Marine Mammal Stranding Network, in conjunction with the North Carolina Wildlife Resources Committee, from deceased (standard Code 2, Geraci and Lounsbury 2005) individuals stranded in 2011 along the outer banks of North Carolina. The tissues were requested pursuant to a letter of authorization under 50 CFR 216.22 and 216.37 of the Marine Mammal Protection Act through the National Marine Fisheries Service (Permit #17530, Appendix A) issued to Andreas Fahlman, Ph.D. and obtained in conjunction of grant funding by the US Naval Service. All specimens were preserved in a 10% formalin solution and shipped to Texas A&M University-Corpus Christi.

Three tracheae from white-tailed deer (*Odocoileus virginianus*) were obtained from Nueces County, Texas from animals taken by hunters during legal hunting seasons between 2012 and 2013. One of the tracheae was obtained fresh whereas the other two were frozen prior to being preserved in a 10% neutral buffered formalin solution. Because these tracheae were obtained from animals taken by hunters during a regular hunting season, their possession required no formal or institutional permits.

Data Collection

All tracheae (Appendix B) were photographed and measured after they were preserved and prior to further manipulation. After whole specimens were preserved and measured, extraneous tissue surrounding the tracheae was excised to expose the tracheal rings. The tracheae were then trimmed for length with the proximal region (most anterior) beginning at the first cartilaginous ring following the cricoid cartilage and ending with the tracheal carina immediately anterior to bronchial separation of the left and right primary bronchi. The tracheae were then measured for the anterior-posterior length.

To determine regions, the most cranial surface was chosen for the proximal region for microtome sectioning, while the most caudal surface represented the distal region. The midpoint (total length/2) was transversely cut between proximal and distal surfaces (after excision of extraneous length) and represented the medial region (Fig. 3). The regions were designated “Proximal” (P), “Medial” (M) and “Distal” (D) for future reference with each trachea. Medial regions were measured for tracheal width and lumen width for each specimen; and then could be sampled from either cranial or caudal portions of the tracheae; however, the surface closest to the transverse cut was selected for microtome sectioning to maintain continuity and reliability.

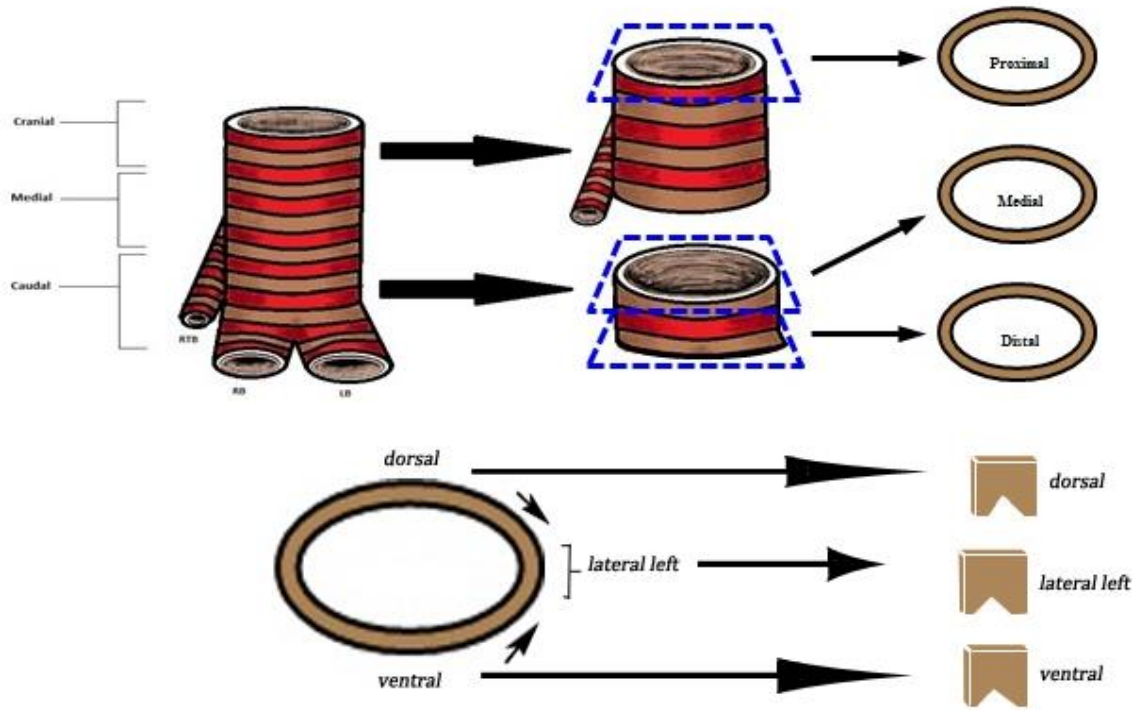


Figure 3. Defining dolphin tracheal regions and subregions. Cranial terminus was designated “Proximal”, caudal surface was designated “Distal” and the surfaces closest to the midline transverse cut were designated “Medial”. Subregions were defined as the dorsal and ventral regions. The lateral left subregion was chosen to avoid complications due to a *bronchus trachealis* (RTB) in odontocete tracheae, which was separate from the right (RB) and left (LB) primary bronchi.

To determine subregions, the orientation of the tracheae were visualized in cross section and were determined to be dorsal, ventral and lateral left (chosen to prevent complication of the right tracheal bronchus in *Tursiops truncatus*). These regions were chosen as close to center of the tracheal mass for these subregions to be consistent throughout experimental procedure. Dorsal and ventral subregions were opposite sides of the minor elliptical axis long the sagittal plane of the trachea. The lateral left subregion was chosen as the midpoint between the dorsal and ventral midlines along the left circumference. The subregions were then designated “dorsal” (d), “ventral” (v) and “lateral left” (l’).

At these predetermined regions and subregions, 0.5 cm x 0.5 cm square sections were removed from the tissue (thickness was determined by trachea itself). A small 2.0 mm “V”-shaped divot was cut

into the tissue opposite of the eventual cutting surface to preserve orientation. All samples were designated with a capital letter for region, while subregions were labeled with a lower-case letter making for clear identifications (Regions: “P” for proximal, “M” for medial, “D” for distal; subregions: “d” for dorsal, “v” for ventral and “l” for lateral left). Region/subregion combinations were designated “Proximal dorsal” (Pd), “Proximal ventral” (Pv), “Proximal lateral left” (Pl), “Medial dorsal” (Md), “Medial ventral” (Mv), “Medial lateral left” (Ml), “Distal dorsal” (Dd), “Distal ventral” (Dv) and “Distal lateral left” (Dl).

Samples were dehydrated in increasing concentrations of ethanol (30%, 50%, 70%, 95% and 100%), cleared with Histo-Clear (d-limonene; National Diagnostics Atlanta, GA USA) and embedded in Paraplast Plus (Sigma-Aldrich Company St. Louis, MO USA). Embedded tissue was sectioned at 7 μ m using a rotary microtome, affixed to glass slides with Mayer’s albumin (DeGiusti and Ezman 1955). Sections on the slides were decerated using Histo-Clear, rehydrated through a graded series of ethanol solutions and stained using an elastic tissue stain (Weigert 1898, Sheehan and Hrapchak 1980) consisting of hematoxylin and eosin (H & E) along with Weigert’s resorcin/fuchsin and a Van Giesen counterstain (McManus 1950). Stained sections were then dehydrated through an ethanol series and finally cleared with Xylene for 10 minutes and coverslipped using Permount mounting medium (Fisher Scientific, Fair Lawn, NJ USA).

Permanent slides were then photographed with an Olympus[®] SZ-PT digital camera with a SZ60 lens (Olympus America Inc. Melville, NY USA) mounted in a VistaVision™ Compound Microscope V166035 (VWR Scientific Products West Chester, PA USA) and recorded via Spot Basic software v3.0.1 (Diagnostic Instruments, Inc. Sterling Heights, MI USA). Linear distances on the images were calibrated using a stage micrometer.

Elastin occurs within the submucosa of the trachea, between the epidermis and the tracheal cartilages. Initial observations indicated that the thickness of the submucosa varies from specimen to specimen. Rather than use a consistent area as the field of measurement (and possibly excluding some of

the submucosa from or including adjacent epithelium or cartilage in the field), the field measurement was determined by the thickness of the submucosa. To measure the percent coverage of elastin across the entire submucosa, the distance from the free surface of the epithelium to the perichondrium of the tracheal cartilage (or the trachealis muscle in the dorsal subregion of *Odocoileus virginianus* trachea) was measured and this value was used as the size of a side in a square field of measurement. This raised issues as the epithelial surface is not a straight line, and an effort was made to select fields that included minimal epithelial undulations. Subsequently, the images were cropped to create a square image (“Analysis Sample Region”; Fig. 4) to eliminate confounding variables. The area of analysis was uniquely sampled to provide the best example of a linear epithelial surface to maximize the Analysis Sample Region and limit lumen coverage, providing the best evaluation of elastin abundance within the tissue.

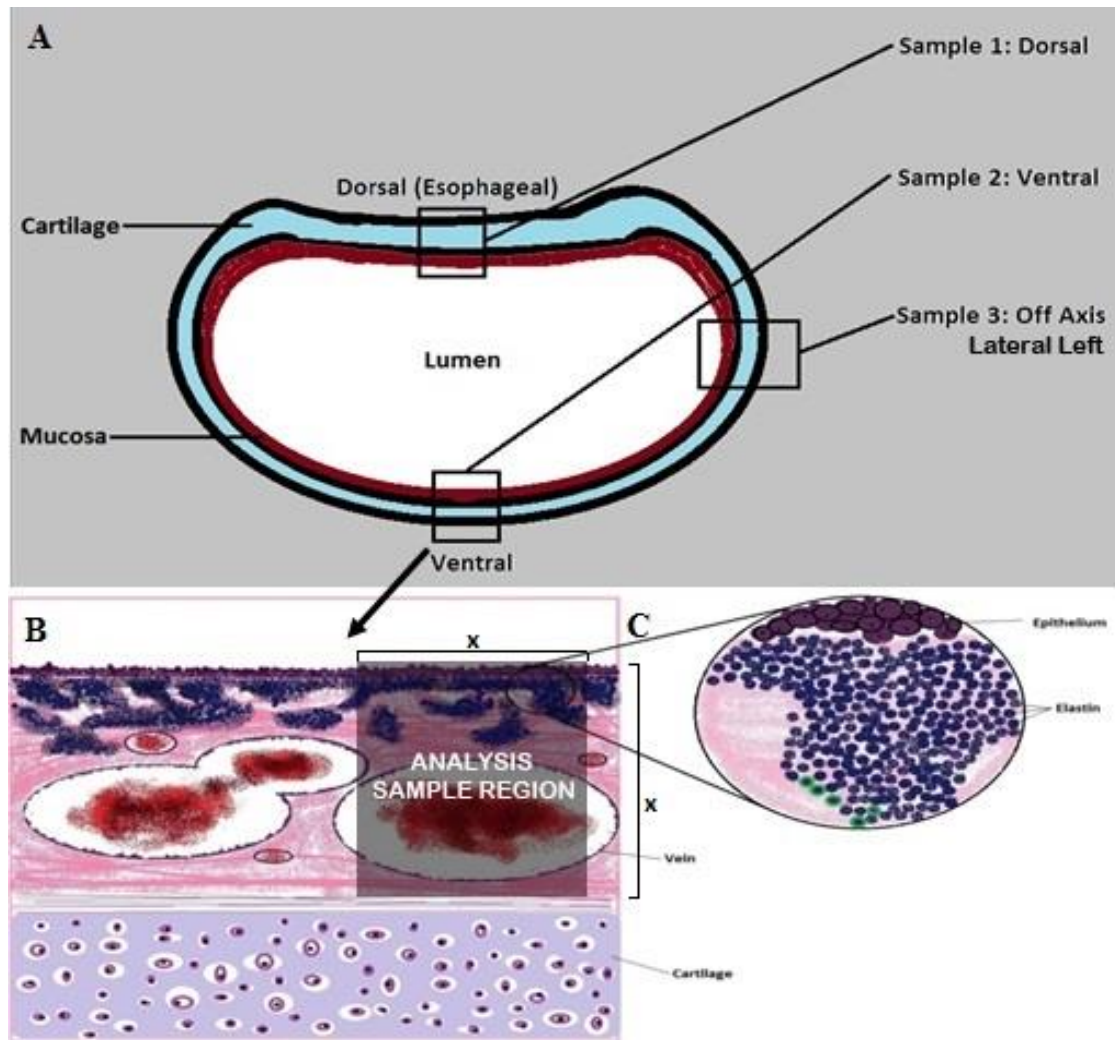


Figure 4. Example of subsection regionalization. Sampling area (A) and determination of subregionality. Illustration of the an example slide (B) exemplifying how the depth from luminal surface (x) was used to determine an “Analysis Sample Region” extending from the luminal epithelial edge down to the perichondrium. An illustration of the blue-black staining of elastin groupings (inset C) exemplifies calculable elastin fibers in the overall quantification.

Sharpness and color of images were then adjusted to accentuate the elastic fibers using Adobe Photoshop™ CS5 (Adobe Systems Incorporated 2010) and analyzed using an ImageJ 1.47v software package (Schneider et al. 2012) to quantify elastin content of the tracheal sections (Fig. 5).

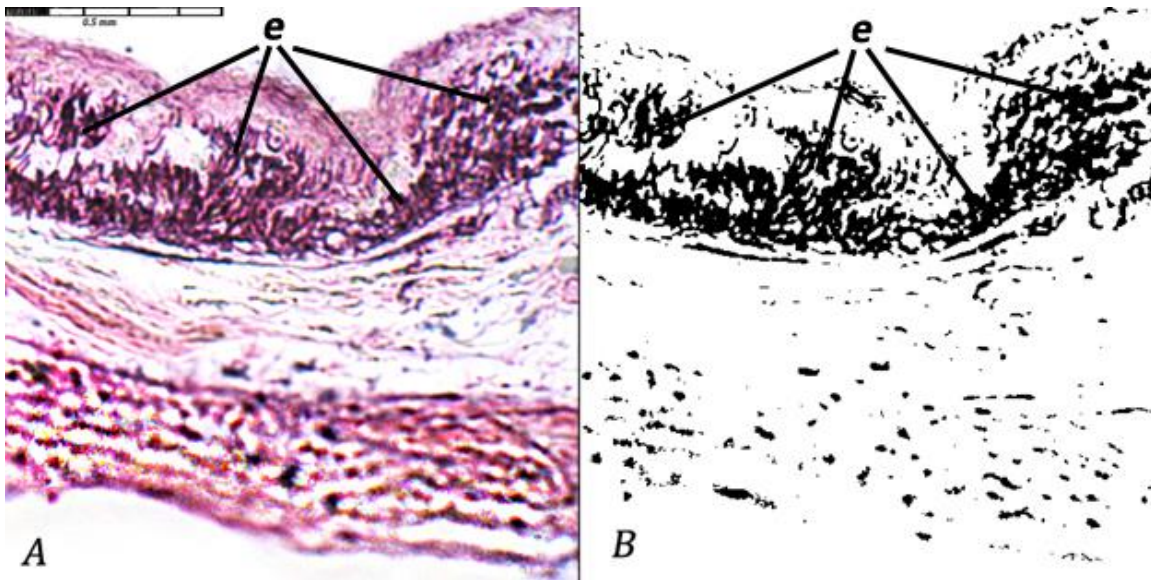


Figure 5. Example of adjusting photomicrographs. Tracheal elastin within a bottlenose dolphin (A) visualized via Adobe Photoshop™ CS5, to exhibit pixel luminosity of less than 87 (on a range of 0=black to 255=white) distinguishing the characteristic blue-black color of the resorcin-fuchsin stain upon the elastin (e) fibers (B).

Individual elastic strands proved difficult to count using a modified plug-in for cell counting program therefore a calculated total proportion of elastin was used for the entire analyzed image (for consistency) after threshold (0-87 on a scale of pixel luminosity) and sample area size parameters are set using the aforementioned software package(s). This novel thresholding technique and range had the advantage of selecting the distinct blue-black of Weigert's resorcin-fuchsin stain, which only stained the elastic fibers, and allowed for the elimination of lighter stained structures. This method was chosen due to the level of compaction and unknown orientation of the elastin fibers which prevented individual "strand" counting. Additionally, the intensity and dark color of the resorcin-fuchsin stain made this the most practical technique for this study (Fig. 6).

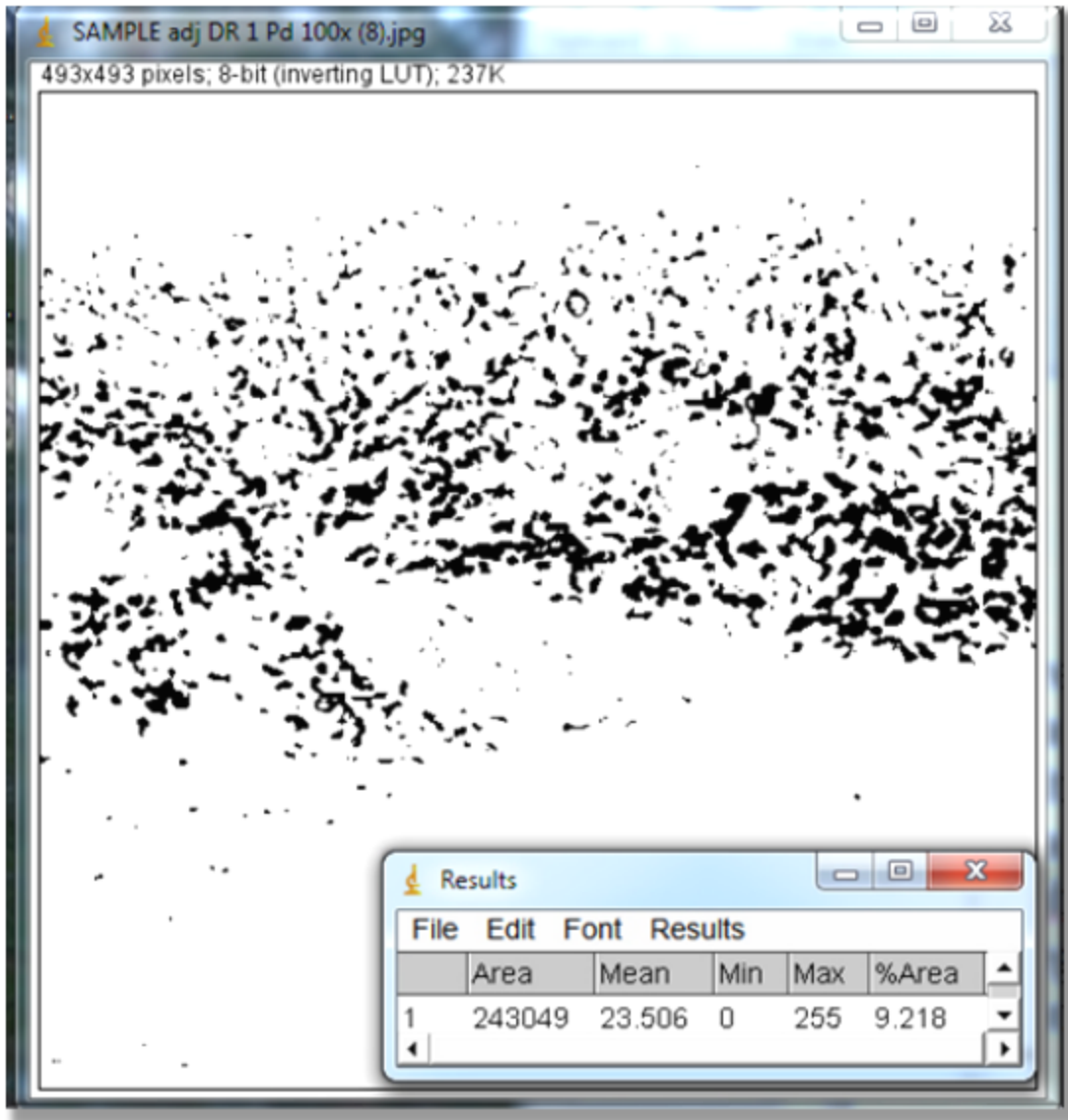


Figure 6. Determining proportional data value from a thresholded image. The program calculated the amount of dark pixels on the image against the whole image area and generates a proportional value (9.218%).

Data Analysis

Values for elastin were calculated as percent of total coverage and were collected from each region/subregion combination per specimen (a minimum of three values for each specimen) and recorded. All regional values (e.g., Pd, Pv, and Pl) were averaged to determine the species regional mean (e.g.,

Proximal region). Likewise, all subregional values (e.g., Pd, Md, and Dd) were averaged for the species subregional mean (e.g., dorsal subregion). All values for region and subregion (e.g., Pd, Pl, Pv, Md, Ml, Mv, Dd, Dl, Dv) were combined for the overall mean per specimen (e.g., DR001). These calculations were done for every specimen (Appendix C) and used to develop species mean values for comparison.

An initial hypothesis was that there might be differences in elastin abundances among the defined subregions and/or regions. To address this hypothesis, after the values were aggregated it was necessary to determine if there were differences in elastin abundance among subregions and regions. If there were differences either among subregions or regions, or an interaction, then each region and subregion by species would have to be analyzed separately. After determining that the data were normally distributed (Appendix D), a 2-way ANOVA was run to determine if there were significant differences between subregions, regions, or if the interaction of regions and subregions was significant. Because there were no significant differences within or between factors (Appendix E), the data could be aggregated for analysis into a single value for elastin percentages for each animal. These data were then used to compare elastin abundances between the species using a Mann-Whitney *U* test.

RESULTS

General tracheal characteristics

Comparison of the tracheae of *Odocoileus virginianus* (terrestrial) and *Tursiops truncatus* (marine) revealed structural differences (Fig. 8). *Odocoileus virginianus* tracheae consisted of a single tube from cricoid cartilage to carina. Conversely, *Tursiops truncatus* tracheae had an additional right tracheal bronchus (bronchus trachealis). *Odocoileus virginianus* tracheae consisted of 45.0 (SE \pm 0.6) (Appendix B) stacked and aligned “C” shaped cartilaginous rings where the tips of the “C” shape were connected by a fleshy trachealis muscle in the dorsal subregion adjacent to the esophagus. The area of the trachea unsupported by cartilage (*paries membranaceus*) has a trachealis muscle contiguous with the cartilage of other subregions. Width of the tracheal lumen was also consistent (2.3 cm, SE \pm 0.1 cm) (Appendix B) through all three specimens despite variations in tracheal length (24.4 cm, SE \pm 10.2 cm) (Appendix B).

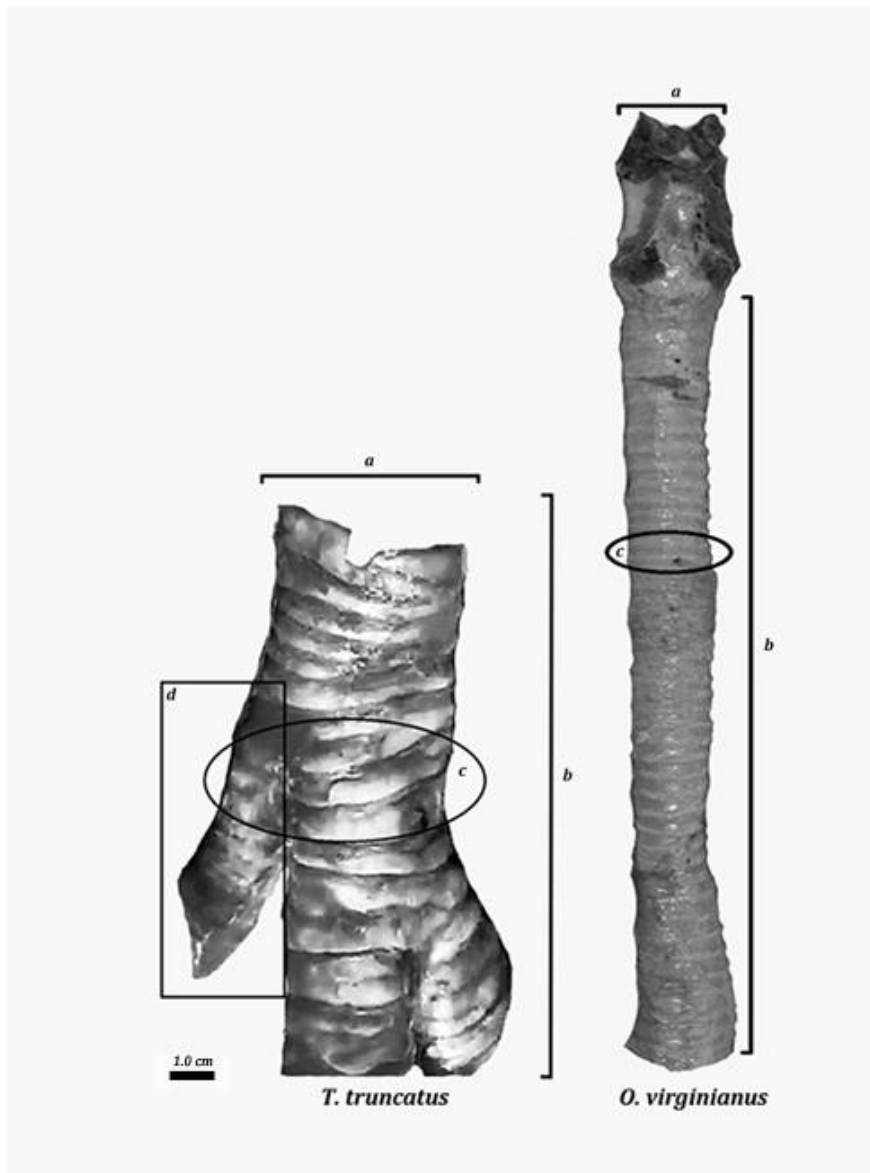


Figure 7. Tracheal differences in gross anatomy. Atlantic bottlenose dolphin (*Tursiops truncatus*) trachea compared to the white-tailed deer (*Odocoileus virginianus*). Differences in tracheal width (a) and length (b). The cartilaginous rings (c, right) in the deer are independent from one another as opposed to the 12 anastomosing irregular shaped rings (c, left) in the bottlenose dolphin. The odontocete trachea has an additional bronchus (*bronchus trachealis*; d).

Tursiops truncatus tracheae also showed complete circumferential cartilaginous rings of inconsistent width along the length of the tracheae. The number of tracheal rings averaged 12.1 (SE \pm 2.2) in the *Tursiops truncatus* from the cricoid cartilage to the carina (Appendix B). There was no *paries membranaceus* in *Tursiops truncatus* since the rings were complete in the dorsal subregion adjacent to the esophagus. The tracheal rings qualitatively varied in width within the same ring and among adjacent rings. Width of the tracheal lumen (measured at the medial region) varied greatly from one *Tursiops truncatus* to the next (3.2 cm, SE \pm 0.4 cm) relative to the overall size of the specimen (Appendix B), while length of the trachea also varied greatly, but was always much shorter than the *Odocoileus virginianus* tracheae (12.1 cm, SE \pm .2.2 cm).

All tracheal rings of *Odocoileus virginianus* were independent from one another, whereas some of the cartilaginous rings of *Tursiops truncatus* featured anastomoses. This association of the rings was consistent across all of the tracheae of *Tursiops truncatus* that were examined

Fine Morphology of the Trachea

Each of the examined species possessed a layer of hyaline cartilage in the external area of the examined sections with the exception of the dorsal subregion in the *Odocoileus virginianus*, which contained a smooth muscle layer (Fig. 9) coinciding with the *paries membranaceus*. The hyaline cartilage was surrounded by a perichondrium separating the cartilaginous ring from the submucosa.

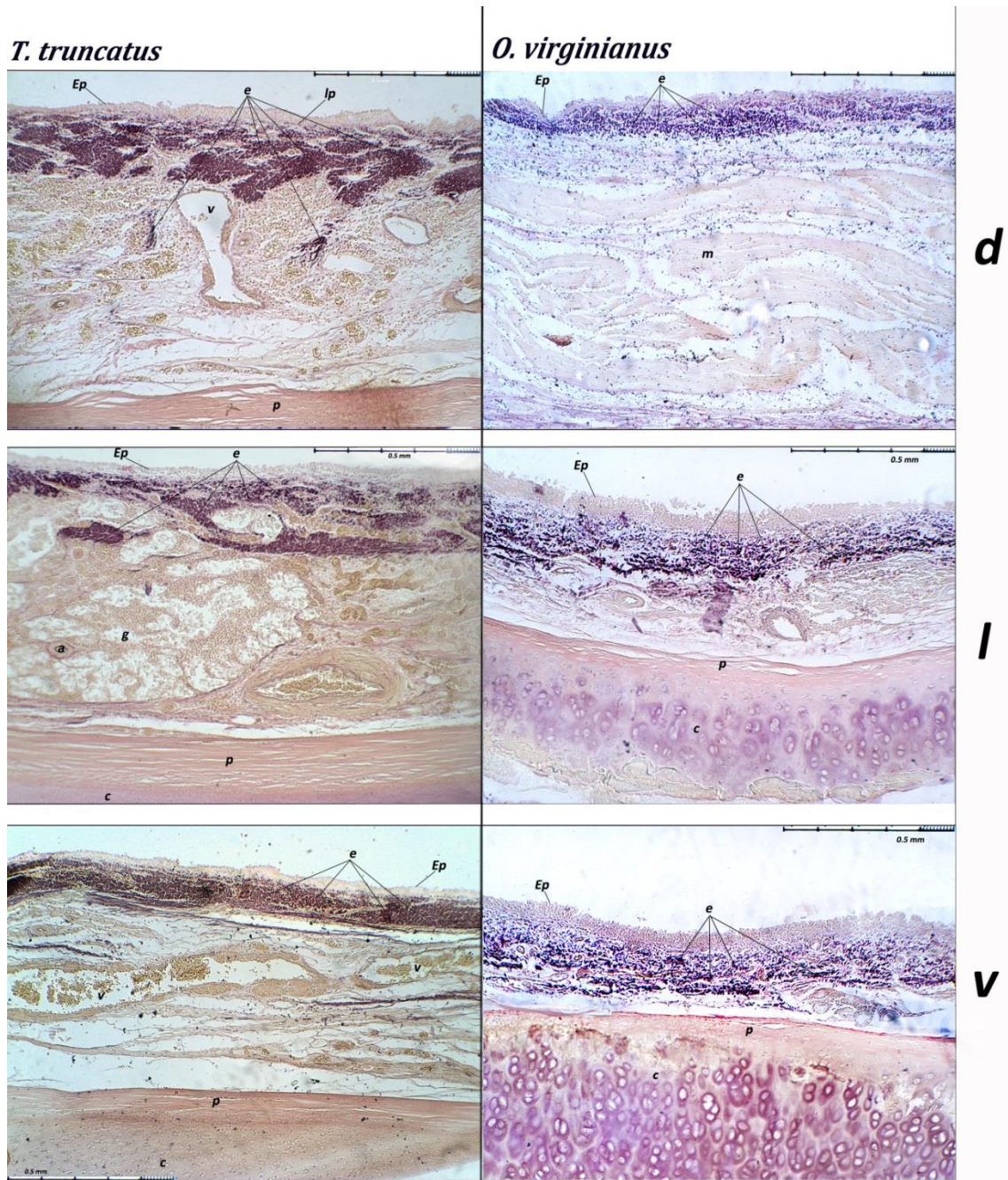


Figure 8. Examples of subregional tissue sections in the two species. The subregional sections (d=dorsal, l=lateral left, v=ventral) compare the abundance of elastin (e) and pattern. The tracheae of both species contained common structures of cartilage (c), perichondrium (p) and epithelial lining (Ep). *Tursiops truncatus* sections contained large venous lacunae (v) and small arterioles (a). *Odocoileus virginianus* exhibited smooth muscle (m) in the dorsal (d) subregion, which was not found in *Tursiops truncatus*.

In the external region of the submucosa, small oval arterioles and irregularly shaped venules were surrounded by dense fibrous connective tissue. In this same region, sparse amounts of elastin were observed, though not consistently. These isolated strands appeared to have a circumferential orientation to the trachea, as opposed to the more compact elastic fibers closer to the lumen.

Tursiops truncatus submucosa tissue housed large thin-walled venous lacunae. These blood vessels were larger than any other structure in mucosa or submucosa; frequently extending beyond the boundary of the observed field. These blood vessels were found in every region and subregion. The lacunae appeared laterally flattened and collapsed with their major axis parallel to the epithelium. No blood vessels of similar size were observed in *Odocoileus virginianus* sections, though smaller arterioles and venules were present in both species.

The inner region of the submucosa also contained mucus and serous glands. These glands were found in both species in the superficial submucosa and were located in the most densely populated region of elastin fibers (Fig. 10). The elastic region in both species was consistently located at the innermost submucosal region. The elastic fibers of *Odocoileus virginianus* were sparse and individual fibers seemed independent, whereas the elastin fibers of *Tursiops truncatus* were so closely associated that individual fibers could only be discerned at the peripheral edges of the elastin clusters. The elastin fiber pattern described for each species was consistent across all regions and subregions of the tracheae examined.

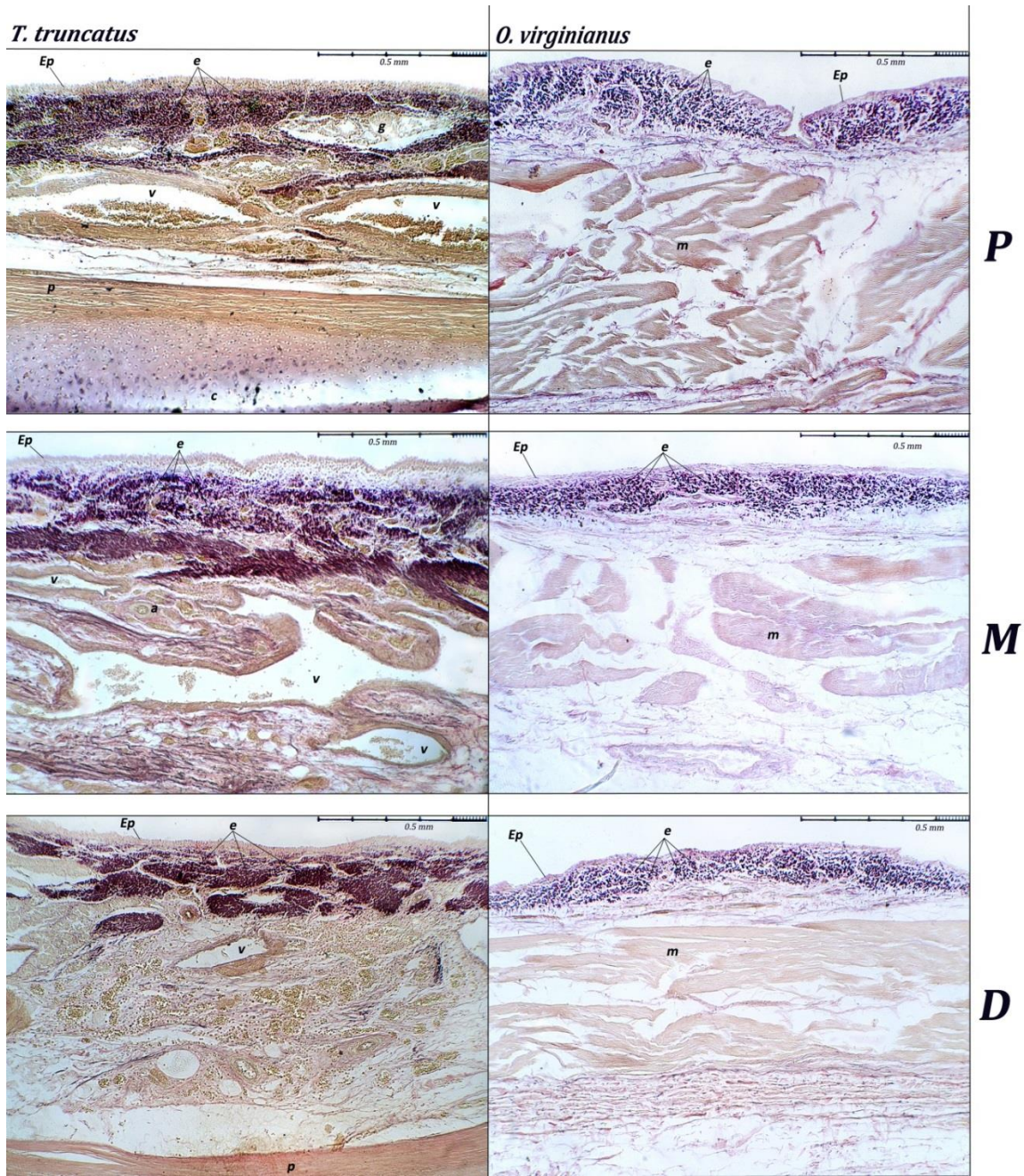


Figure 9. Fine structure tracheal differences between species. *Odocoileus virginianus* and *Tursiops truncatus* with proximal (P), medial (M) and distal (D) regions. Sections show variations in types of epithelium (Ep) and elastin grouping. Blood vessels venous lacunae (v) and arterioles (a) were identified. Smooth muscle (m) was only found in *Odocoileus virginianus*. Both species contained hyaline cartilage (c) lined by a perichondrium (p).

The epithelium of *Odocoileus virginianus* appeared orderly and consistent within all observed sections, while the epithelium of *Tursiops truncatus* was observed as a series of rounded apices along the lumen, appearing irregular and unevenly spaced (Fig. 11).

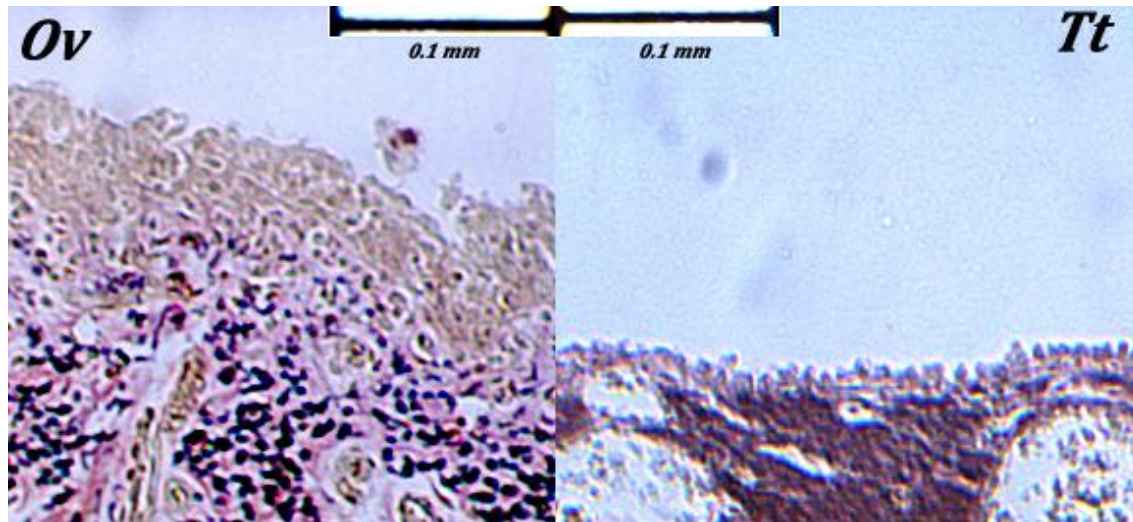


Figure 10. Epithelium of *O. virginianus* (Ov) and the *T. truncatus* (Tt). The epithelium on the right shows multiple layers (stratification) whereas the epithelial layer of *Tursiops truncatus* on the right exhibits cells with rounded apical surfaces, indicative of transitional epithelium.

Elastin Coverage and Distribution

Elastin fibers in *Odocoileus virginianus* were found only sporadically throughout the upper superficial submucosa indicating limited organization and inter-fiber association. Compared to *Odocoileus virginianus*, elastin fibers in tracheae of *Tursiops truncatus* appeared densely grouped and compacted (Fig. 12).

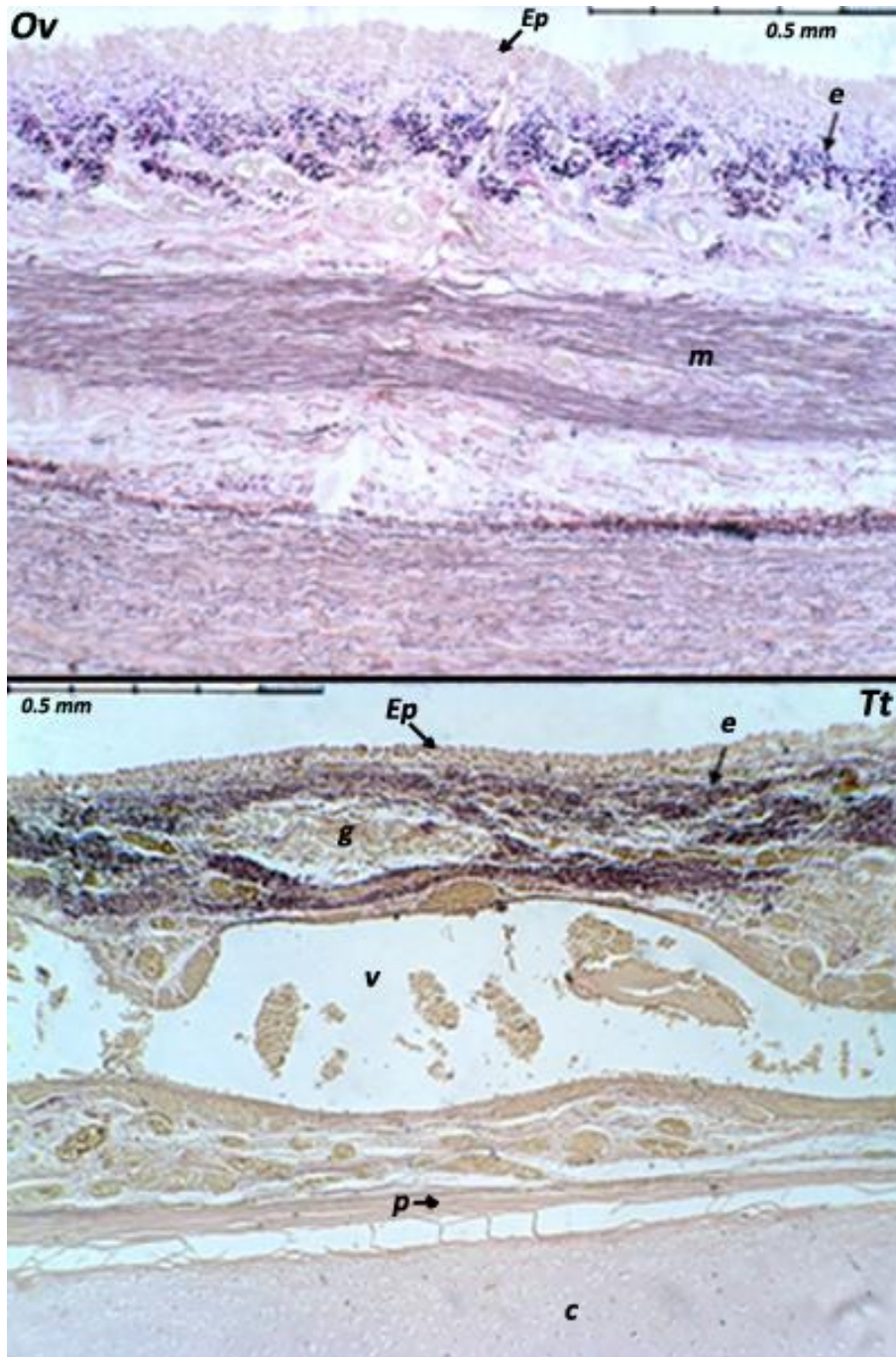


Figure 11. Comparison of Distal/dorsal (Dd) tracheal tissues in two mammalian species (Ov – *Odocoileus virginianus* and Tt – *Tursiops truncatus*). The elastic fibers (e) show different degrees of grouping beneath the epithelium (Ep). Hyaline cartilage (c) surrounded by perichondrium (p) and large venous lacunae (v) are seen in the regions of *Tursiops truncatus* (below), but *Odocoileus virginianus* has a muscular trachealis (m) layer. Each of the sections in the figure was stained with hematoxylin & eosin to show tissue differentiation and then stained with Weigert’s Elastic stain to present the blue-black elastin fibers.

In *Tursiops truncatus*, venous lacunae were found in the submucosa. These blood vessels appeared thin-walled and without elastic fiber content, yet were adjacent to the elastin fiber bundles. The size of these blood vessels occasionally extended beyond the width of the tissue sections (approximately 1.5 mm) and appeared amorphous compared to the much smaller oval arterioles.

Elastin content evaluation

Regardless of whether the coverage of elastin fibers was considered at the subregion or region (Table 1), elastin coverage was greater in *Tursiops truncatus*, with an overall mean of 8.9% (SE \pm 0.2) compared to 7.0% (SE \pm 0.2) in *Odocoileus virginianus* (Figure 14). The Mann-Whitney *U*-test ($\alpha = 0.05$) was used to compare the mean elastin coverage of *Odocoileus virginianus* and *Tursiops truncatus*. Elastin coverage in *Tursiops truncatus* was significantly greater than in *Odocoileus virginianus* (df = 8, *U* = 0; *P* = 0.0167).

Table 1. Mean values for elastin coverage (%) were determined for each region/subregion combination by species. Proximal dorsal (Pd), Proximal lateral left (Pl), Proximal ventral (Pv), Medial dorsal (Md), Medial lateral left (Ml), Medial ventral (Mv), Distal dorsal (Dd), Distal lateral left (Dl), Distal ventral (Dv) for each individual were combined for species (*Tursiops truncatus*, *n*=7; *Odocoileus virginianus*, *n*=3).

Species		Pd	Pl	Pv	Md	Ml	Mv	Dd	Dl	Dv
<i>O. virginianus</i>	Mean	6.4	6.9	6.9	6.3	6.7	7.8	7.4	7.3	6.5
	SE	0.3	1.0	0.6	0.3	0.6	0.1	0.7	0.7	1.1
<i>T. truncatus</i>	Mean	9.3	8.7	7.7	9.4	9.0	8.9	8.9	9.5	9.4
	SE	0.4	0.4	0.4	0.8	0.7	0.7	0.5	0.7	1.0

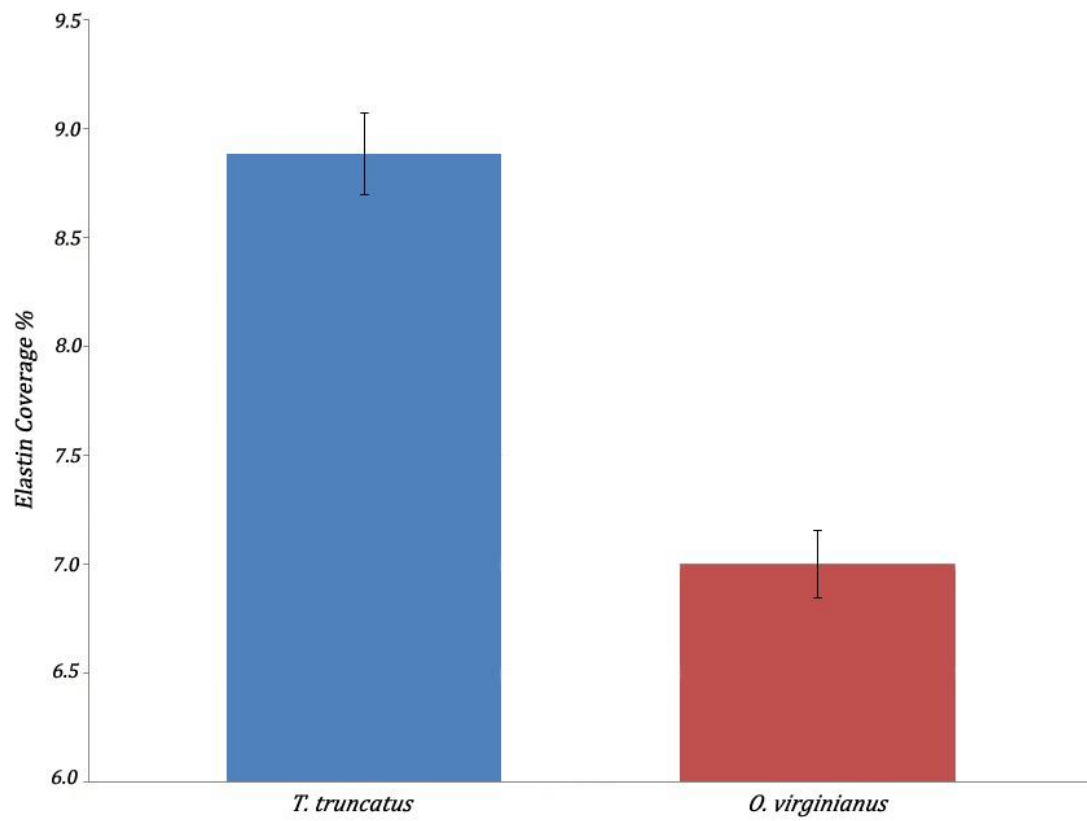


Figure 12. Overall means of elastin coverage with standard error bars for each species.

DISCUSSION

Until recently, very few studies have examined the role the trachea plays in diving, and even fewer studies have compared tracheae between species with lifestyles that alter the essential functions of these airspaces (Bagnoli et al. 2011). While their precise taxonomic relationship is in dispute (Arnason et al. 2004, Price et al. 2005), the clades to which the two species examined in this study belong (i.e., artiodactyls for *Odocoileus virginianus* and cetaceans for *Tursiops truncatus*) evolved from a common terrestrial ancestor. Because elastin is often responsible for retaining the conformation of tissues during and after the application of stress, understanding its role in maintaining tracheal function during diving behavior is important to understanding the broader suite of diving adaptations in marine mammals (Yang 2008). To date, no studies have quantified or compared elastin abundance in mammalian tracheae.

In this study, I elucidate several differences in the gross morphology of the tracheae including tracheal dimensions, tracheal architecture, and cartilaginous ring structure. In addition, I document significantly greater coverage of elastin fibers in *Tursiops truncatus* tracheae than in those of *Odocoileus virginianus*.

Gross Morphology

The trachea of *Odocoileus virginianus* is a single, long, narrow tube with numerous “C”-shaped cartilaginous supports whose tips are connected by the *paries membranaceus*. The *paries membranaceus* contains the trachealis muscle, whose cells are arranged in transversely and longitudinally oriented bundles (Kamel 2009, Bagnoli et al. 2011). Contraction of the longitudinal bundles dilates the trachea to facilitate forceful expulsion of foreign materials and/or mucus. The trachealis muscle also dilates the trachea to accommodate food passing through the esophagus while swallowing and rumination (Kamel et al. 2009). Individual tracheal cartilages in *Odocoileus virginianus* are thinner (cranio-caudally) compared to those of *Tursiops truncatus*, and show no cartilaginous connections to one another.

The trachea of *Tursiops truncatus* is shorter and wider than that of *Odocoileus virginianus*, and exhibits a third bronchus on the right side. The cartilaginous tracheal supports are “O”-shaped (and therefore lack *paries membranaceus*), wide, irregular, and often described as “plates” when compared to the appearance of such supports in terrestrial mammals (Fanning 1977, Davenport 2009, Bagnoli et al. 2011). Tracheal rings firmly attach to adjacent rings by cartilaginous anastomoses (Appendix F), connections that increase tracheal stiffness and rigidity. Cozzi et al. (2005) compared tracheal mechanical properties between striped dolphins (*Stenella coeruleoalba*) and terrestrial mammals, and provided evidence that complete cartilaginous rings and anastomoses stiffened the trachea and increased its resistance to mechanical failure. Even though reinforced by anastomoses, the trachea remains flexible, allowing “spiraled” cranio-caudal expansion and contraction during ventilation (Moore et al. 2014). Furthermore, not all odontocete tracheal rings anastomose; individual odontocetes may exhibit tracheal ring independence in the first few tracheal cartilages immediately caudal to the cricoid cartilage (Fanning 1977).

The presence of an accessory bronchus (*bronchus trachealis*) in *Tursiops truncatus* provides an additional respiratory airway to handle a greater volume of air. The combined volume of the *bronchus trachealis* and the right bronchus exceeds the volume of the left bronchus (Cozzi et al. 1994). However, the right accessory bronchus is also found in some terrestrial mammals (e.g., domestic swine, *Sus scrofa*), so it is uncertain whether it represents a derived character or an ancestral character (Moore et al. 2014).

For the specimens used in this study, the tracheae of *Tursiops truncatus* were approximately half the length of those of *Odocoileus virginianus*, and contained one-third the number of cartilaginous supports. Cartilaginous rings in *Tursiops truncatus* were approximately one-and-one-half times as wide as those of *Odocoileus virginianus*. These differences in gross morphology represent adaptations for flexibility, protection from damage, and efficient ventilation.

Odocoileus virginianus is a terrestrial grazer, experiencing minimal ambient pressure changes. *Odocoileus virginianus* have reliable, consistent access to air, and their ventilatory rhythms are regular. Their tracheae are adapted for flexibility and increased range of motion. Long, narrow tracheae with numerous small, independent cartilaginous rings provide adequate structural support for maintaining a patent airway, while facilitating cervical movement in multiple axes.

Tursiops truncatus is a marine mammal that regularly dives to depths greater than 100 m (Rommel et al. 1990). As a result, *Tursiops truncatus* experience extensive pressure variation compared to terrestrial species. The cranium and cervical vertebrae are cranio-caudally compressed, which restricts the range of motion in the “neck.” The cartilaginous rings have broadened and anastomosed to form a rigid architecture that resists external pressures. As divers, *Tursiops truncatus* must respire infrequently. They exchange more than 80% of their lung capacity in 0.5 seconds during each ventilatory cycle (Scholander 1940, Irving et al. 1941). Increased tracheal volume facilitates the rapid air flow during ventilation.

Fine Structure

The fine structure of the trachea in both species exhibited many common components (e.g., small blood vessels and various glands). Elastin fibers were found consistently in the upper (closest to the lumen) submucosa in both species. In general appearance, the elastin fibers of *Odocoileus virginianus* appeared to be more widely separated from one another, while the elastin fibers of *Tursiops truncatus* were more tightly packed together (Appendix G). The fine structure of the layers of the tracheal wall correspond closely to the “standard” described in human histology textbooks and in other terrestrial mammals (Fanning and Harrison 1974, Kamel et al. 2009, Bagnoli et al. 2011). For example, the ciliated pseudostratified epithelium that I observed in *Odocoileus virginianus* was also noted by Brooks (2010), and the motion of these cilia help to remove debris from the respiratory tract.

The tracheal epithelium of *Tursiops truncatus* resembles transitional epithelium. This type of epithelium has been reported in other odontocete tracheae (Fanning and Harrison 1974, Fanning 1977).

The presence of transitional epithelium is associated with structures that undergo extensive, temporary expansion and contraction. Cilia are not present in *Tursiops truncatus* though microvilli have been reported (Fanning and Harrison 1974). Fanning (1977) postulated that debris removal in odontocete tracheae occurs by “gravity and mucus flow”, directing materials toward the larynx to expel the material with deliberate, forceful exhalations, called “chuffing.”

Function of vascular plexus and associated elastic fibers

The submucosa of *Tursiops truncatus* tracheae contained large, thin walled venous lacunae. These blood vessels form a vascular plexus running longitudinally within the tracheal submucosa. A large concentration of elastin fibers are adjacent to this vascular plexus, and a similar arrangement has been reported in other odontocetes (Fanning and Harrison 1974, Fanning 1977, Cozzi et al. 2005, Bagnoli et al. 2011, Davenport et al. 2013).

Attributes of *Tursiops truncatus* tracheal morphology observed in this study provided insight into tracheal function during diving and surfacing. The venous plexus is able to engorge with blood and expand—in a manner similar to erectile tissue in the mammalian reproductive system (Fanning and Harrison 1974, Fanning 1977, Cozzi et al. 2005, Piscitelli et al. 2010, Bagnoli et al. 2011). The abundance of tracheal elastin allows a rapid draining of the blood from the venous plexus as *Tursiops truncatus* surfaces. For the trachea, the “resolution phase” of the submucosal tissue must be rapid in order to clear the airway by the time *Tursiops truncatus* break the surface to breathe. A transitional-type epithelium is consistent with accommodating these rapid changes in the tracheal structure during diving and surfacing.

In 1973, Kooyman examined x-ray images of a Weddell seal (*Leptonychotes weddellii*) taken during a hyperbaric forced diving experiment. The x-rays visualized and recorded the collapse the pinniped trachea at simulated depth. Cozzi et al. (2005) suggested that expansion of vessels in its submucosal vascular plexus would provide internal support for the trachea. Additionally, the expansion of the submucosal tissue would decrease the volume of the trachea, and air in the trachea would be under

increased pressure. As the odontocete returned to the surface and external pressure decreased, the air trapped in the trachea would expand, assisting with the draining of blood from the engorged vascular plexus, and helping to return the trachea to its normal conformation. Elasticity of the tracheal mucosa and submucosa (due to the presence of elastin) would also assist in the process of returning the airway's patency (Yang 2008).

Similar tracheal adaptations were described in leatherback sea turtles (*Dermochelys coriacea*) by Davenport et al. (2009). In addition to supporting the trachea against external pressure, they provide two additional functions of a vascularized tracheal lining: 1) inspired air would be warmed and/or humidified for respiration when passing over the vascularized tissue (both sea turtles and odontocetes lack turbinate bones); and 2) even when the tissues were engorged with blood, there would be a patent tracheal lumen which could act as an air reservoir. The idea that the trachea acts as an air reservoir when the lungs collapse during a deep dive was first put forth by Scholander (1940). Scholander also suggested that the compressed air in the trachea would expand during surfacing and assist in re-inflating the lungs as the animal rises in the water column. The expanding air in the tracheal reservoir also helps to force the blood from the venous plexus and widen the airway prior to the animal taking a breath at the surface.

Future Directions

Documenting the orientation, association, and arrangement of elastin fibers would enhance the understanding of elastin's role in tracheal compliance. A simple modification to the techniques used in this study (e.g., using the Weigert's resorcin/fuchsin stain either with a light counterstain or no counterstain) would accentuate the elastin "signal," and eliminate much of the "background noise." Use of anti-elastin antibodies and immunohistochemical techniques (viewed through a light, fluorescence or confocal microscope) would have a similar benefit. A higher signal-to-noise ratio would reduce the need for thresholding the digital images, and also allow increased reliability of elastin identification. Additionally, clearing and staining methods have been developed that allow small blocks of tissue whose components have been marked using chemical or immunohistochemical protocols to be

viewed in three dimensions (Klymkowsky and Hanken, 1991). Such cleared and stained “whole mounts” are a direct way to view the three-dimensional orientation of the elastin fibers. A more time-consuming way of reconstructing the three-dimensional orientation of the elastin fibers would be to combine digital photographs of serial sections through the tissue using three-dimensional reconstruction software.

In this study, I normalized the amount of elastin as percent coverage of a cross-sectional area. Improved staining and imaging techniques (with higher magnification and resolution) could allow the amount of elastin to be quantified directly from serial sections (e.g., as a number of fibers per volume, or volume of elastin per total volume) as a unit of measurement in lieu of a proportional figure. Another direct method of determining the amount of elastin within tracheal tissues could involve digesting away tissue components other than elastin and determining the dry weight of the remaining elastin. Such a protocol (if one exists) would allow for a reliable direct measurement of tracheal elastin while eliminating confounding variables.

Comparisons among several odontocete species could also provide new insights to determine if the results found in *Tursiops truncatus* will generalize to closely related species. Adding odontocetes with various diving habits (e.g., a very deep-diving odontocete) would allow comparisons based on the predicted functions of elastin during the diving process. Such functional correlations need not be restricted to odontocetes, or even to mammals. It would also be beneficial to determine if the observed differences apply to non-mammalian species (e.g., sea turtles vs. terrestrial turtles, marine iguanas vs. terrestrial iguanas).

Finally, a large sample size would allow for more consistency and reliability of results in any of these studies. However, many of the most interesting candidates to use as specimens are endangered, threatened or otherwise protected. To accommodate this, researchers must therefore rely on “windfall” specimens, and sample sizes are likely to remain small.

LITERATURE CITED

- Adobe Systems Incorporated. 2010. Adobe Photoshop CS5: Javascript scripting reference (Revision 1). 345 Park Avenue, San Jose, California 95110, USA.
- Bagnoli, P., B. Cozzi, A. Zaffora, F. Acocella, R. Fumero and M. L. Constantino. 2011. Experimental and computational biomechanical characterization of the tracheo-bronchial tree of the bottlenose dolphin (*Tursiops truncatus*). *Journal of Biomechanics* 44:1040-1045.
- Berta, A., J. L. Sumich and K. M. Kovacs. 2005. Respiration and diving physiology. Pages 299-343 in *Marine Mammals: Evolutionary Biology*. Third Edition. Academic Press, Boston, MA
- Bostrom, B. L., A. Fahlman and D. R. Jones. 2008. Tracheal compression delays collapse during deep diving in marine mammals. *Respiratory Physiology & Neurobiology* 161:298-305.
- Boyden, A., and D. Gemeroy, 1950. The relative position of the Cetacea among the orders of Mammalia as indicated by precipitin tests. *Zoologica* 35:145–151.
- Brooks, J. W. 2010. A comprehensive study of the health of farm-raised whitetailed deer (*Odocoileus virginianus*) with emphasis on respiratory tract infection by *Fusobacterium* spp. Ph.D. dissertation, Pennsylvania State University, University Park, PA. 138 pp.
- Cotten, P. B., M. A. Piscitelli, W. A. McLellan, S. A. Rommel, J. L. Dearolf and D. A. Pabst. 2008. The gross morphology and histochemistry of respiratory muscles in bottlenose dolphins, *Tursiops truncatus*. *Journal of Morphology* 269:1520-1538.
- Cozzi, B., J. D. Mikkelsen, J-P Ravault, A. Locatelli, J. Fahrenkrug, E-T. Zhang and M. Møller. 1994. Density of peptide histidine-isoleucine- and vasoactive intestinal peptide-immunoreactive nerve fibers in the sheep pineal gland is not affected by superior cervical ganglionectomy. *Journal of Comparative Neurology* 343:72-82.
- Cozzi, B., P. Bagnoli, F. Acocella and M. L. Constantino. 2005. Structure and biomechanical properties of the trachea of the striped dolphin *Stenella coeruleoalba*: evidence for evolutionary adaptations to diving. *Anatomical Record part A* 284A:500-510.
- Davenport, J., J. Fraher, E. Fitzgerald, *et al.* 2009. Ontogenetic changes in tracheal structure facilitate deep dives and cold water foraging in adult leatherback sea turtles. *Journal of Experimental Biology*. 212:3440-3447.
- Davenport, J., L. Cotter, E. Rogan, D. Kelliher, and C. Murphy. 2013. Structure, material characteristics and function of the upper respiratory tract of the pygmy sperm whale. *The Journal of experimental biology* 216(24):4639-4646.
- DeGiusti, D. L. and L. Ezman. 1955. Two methods for serial sectioning of arthropods and insects. *Transactions of the American Microscopical Society* 74:197-201.

- Fahlman, A., A. Olszowka, B. Bostrom, and D. R. Jones. 2006. Deep diving mammals: dive behavior and circulatory adjustments contribute to bends avoidance. *Respiratory Physiology & Neurobiology* 153:66-77.
- Falke, K. J., R. D. Hill, J. Qvist, R. C. Schneider, M. Guppy, G. C. Liggins, P. W. Hochachka, R. E. Elliot and W. M. Zapol. 1985. Seal lungs collapse during free diving: evidence from arterial tensions. *Science* 229(4713):556-558.
- Fanning, J. C. 1977. The submicroscopic structure of the dolphin lung. Ph.D. dissertation, University of Adelaide, Adelaide, South Australia. 286 pp.
- Fanning, J. C. and R. J. Harrison. 1974. The structure of the trachea and lungs of the south Australian bottle-nosed dolphin. Pages 231-252 in R. J. Harrison, ed. *Functional Anatomy of Marine Mammals*. Volume 2. Academic Press, London, England.
- Geraci, J. R. and V. J. Lounsbury. 2005. *Marine Mammals Ashore: A field guide for strandings* Second Edition. National Aquarium in Baltimore, MD.
- Gosline, J. M. and R. E. Shadwick. 1996. The mechanical properties of fin whale arteries are explained by novel connective tissue designs. *Journal of Experimental Biology* 199:985-997.
- Houser, D. S., J. Finneran, D. Carder, W. Van Bonn, C. Smith, C. Hoh, R. Mattrey, and S. Ridgway. 2004. Structural and functional imaging of bottlenose dolphin (*Tursiops truncatus*) cranial anatomy. *Journal of Experimental Biology* 207:3657-3665.
- Irwin, D.M. and U. Arnason. 1994. Cytochrome *b* gene of marine mammals: phylogeny and evolution. *Journal Mammalian Evolution* 2:37-55.
- Irving, L., P. F. Scholander and S. W. Grinnell. 1941. The respiration of the porpoise, *Tursiops truncatus*. *Journal of Cellular Biology*. 17:145-168.
- Kamel, S. K., L. E. Beckert and M. D. Stringer. 2009. Novel insights into the elastic and muscular components of the human trachea. *Clinical Anatomy* 22:689-697.
- Klymkowsky, M. W. and J. Hanken. 1991. Whole-mount staining of *Xenopus* and other vertebrates. *Methods in Cell Biology* 36:419-441.
- Kooyman, G. L., and H. T. Andersen. 1969. Deep diving. Pages 65-94 in H. T. Andersen (ed.). *The Biology of Marine Mammals*. Academic Press, New York, NY.
- Kooyman, G. L., D. D. Hammond and J. P. Shroeder. 1970. Bronchograms and tracheograms of seals under pressure. *Science* 169:82-84.
- Kooyman, G. L. 1985. Physiology without restraint in diving mammals. *Marine Mammal Science* 1:166-178.
- Kooyman, G. L. 1989. *Diverse Divers: Physiology and Behaviour*. Springer-Verlag, New York, NY.
- Kooyman, G. L., P. J. Ponganis. 1998. The physiological basis of diving to depth: birds and mammals. *Annual Review of Physiology* 60:19-32.

- McManus, J. F. A. and R. W. Momry. 1961. Staining methods: histologic and histochemical. *Academic Medicine* 36:108.
- Moore, C., M. Moore, S. Trumble, *et al.* 2014. A comparative analysis of marine mammal tracheas. *The Journal of Experimental Biology* 217:1154-1166.
- O'Leary, M.A. and Geisler, J.H. 1999. The position of Cetacea within Mammalia: phylogenetic analysis of morphological data from extinct and extant taxa. *Systematic Biology*, 48:455-490.
- Piscitelli, M. A., W. A. McLellan, S. A. Rommel, J. E. Blum, S. G. Barco, and D. Pabst. 2010. Lung size and thoracic morphology in shallow-and deep-diving cetaceans. *Journal of Morphology* 271:654-673.
- Piscitelli, M. A., S. A. Raverty, M. A. Lillie, and R. E. Shadwick. 2013. A review of cetacean lung morphology and mechanics. *Journal of Morphology* 274:1425-1440.
- Ponganis, P. J. 2011. Diving mammals. *Comprehensive Physiology*. 1:517-535.
- Price, S. A., O. RP Bininda-Emonds, and J. L. Gittleman. 2005. A complete phylogeny of the whales, dolphins and even-toed hoofed mammals (Cetartiodactyla). *Biological Reviews* 80:445-473
- Quinn, G. P. and M. J. Keough. 2011. *Experimental design and data analysis for biologists*. Cambridge University Press, Cambridge, UK.
- R Core Team. 2012. R: A language and environment for statistical computing. R Foundation for Statistical Computing, Vienna, Austria. ISBN 3-900051-07-0, URL <http://www.R-project.org/>
- Reidenberg, J. S., and J. T. Laitman. 1987. Position of the larynx in Odontoceti (toothed whales). *Anatomical Record* 218:98-106.
- Resnick, R., and D. Halliday. 1966. *Physics Parts I and II*. John Wiley & Sons, New York, NY.
- Ridgway, S. H., B. L. Scronce, and J. Kanwisher. 1969. Respiration and deep diving in the bottlenose porpoise. *Science* 166:1651-1654.
- Ridgway, S. H. 1972. *Mammals of the Sea: Biology and Medicine*. Charles C. Thomas, Springfield, Illinois.
- Ridgway, S. H. and R. Howard. 1979. Dolphin lung collapse and intramuscular circulation during free diving: evidence from nitrogen washout. *Science* 206:1182-1183.
- Ridgway, S. H., and C. A. Fenner. 1982. Weight-length relationships of wild-caught and captive Atlantic bottlenose dolphins. *Journal of the American Veterinary Medical Association* 181:1310-1315.
- Romer, A. S., and T. S. Parsons. 1977. *The Vertebrate Body*. WB Saunders Company, Philadelphia, PA.
- Rommel, S., S. Leatherwood, and R. R. Reeves. 1990. *The Bottlenose Dolphin*. Academic Press, Cambridge, MA.

- Rommel, S.A., Pabst, D.A. and McLellan, W.A., 2009. Skull anatomy. Pages 1033-1047 in W. F. Perrin, B. Würsig and J. G. M. Thewissen, eds. *Encyclopedia of Marine Mammals* 2nd edition. Academic Press, San Diego, CA.
- Saunders, D. A. 1988. *Adirondack Mammals*. Syracuse University Press, Syracuse, NY.
- Schmidt-Nielsen, K. 1997. *Animal Physiology: Adaptation and Environment*. Cambridge University Press, Cambridge, MA.
- Schneider, C. A.; Rasband, W. S. & Eliceiri, K. W. 2012. NIH Image to ImageJ: 25 years of image analysis. *Nature Methods* 9:671-675.
- Scholander, P. F. 1940. Hvalradets Skrifter Norske Videnskaps-Akad. Oslo 22:79.
- Sheehan, D.C. and Hrapchak, B.B. 1980. *Theory and Practice of Histotechnology*. Mosby Incorporated, St. Louis, MO.
- Slijper, E. J. 1958. Organ weights and symmetry problems in porpoises and seals. *Archives Néerlandaises de Zoologie* 13:97-113.
- Smith, T. L., B. S. Turnbull and D. F. Cowan. 1999. Morphology of the complex laryngeal gland in the Atlantic bottlenose dolphin, *Tursiops truncatus*. *The Anatomical Record* 254:98-106.
- Snyder, G. K. 1983. Respiratory adaptations in diving mammals. *Respiration Physiology* 54:269-294.
- Song, S. H. 1994. Three dimensional structures of pulmonary elastin; airway VS vascular elastin. *Yonsei Medical Journal* 35:475-475.
- Starcher, B. C. 1986. Elastin and the lung. *Thorax* 41:577-585.
- Tarasoff, F. J., and G. L. Kooyman. 1973. Observations on the anatomy of the respiratory system of the river otter, sea otter, and harp seal. I. The topography, weight, and measurements of the lungs. *Canadian Journal of Zoology* 51:163-170.
- Taylor, M. A. 1994. Stone, bone or blubber? Buoyancy control strategies in aquatic tetrapods. *Mechanics and Physiology of Animal Swimming* 2:151.
- Thiberville, L., S. Moreno-Swirc, T. Vercauteren, E. Peltier, C. Cave and G. B. Heckly. 2007. *In Vivo* imaging of the bronchial wall microstructure using fibered confocal fluorescence microscopy. *American Journal of Respiratory and Critical Care Medicine* 175:22-31.
- Tsang, K.W., R. Kinoshita, N. Rouke, Q. Yuen, W. Hu, and W. K. Lam. 2002. Bronchoscopy of cetaceans. *Journal of Wildlife Diseases* 38:224-227.
- Weigert, C. 1898. Über eine Methode zur Färbung elastischer Fasern. *Zentralblatt für Allgemeine Pathologie und Pathologische Anatomie* 9:289-292.
- Wells, R. S., and M. D. Scott. 1999. Bottlenose dolphin *Tursiops truncatus* (Montagu, 1821). Pages 137-182 in S. H. Ridgway and R. Harrison, eds. *Handbook of Marine Mammals, Volume 6: The Second Book of Dolphins and the Porpoises*. Academic Press, Cambridge, MA.

Yang, L. 2008. Mechanical properties of collagen fibrils and elastic fibers explored by AFM. Ph.D. dissertation, University of Twente, Enschede, Netherlands. 152 pp.

APPENDIX A

Figure A1-A4. National Marine Fisheries Service permit for marine mammal sample acquisition and usage. Tracheae utilized in this study were part of an addendum for respiratory tissue samples transferred to Texas A&M University-Corpus Christi.



UNITED STATES DEPARTMENT OF COMMERCE
National Oceanic and Atmospheric Administration
NATIONAL MARINE FISHERIES SERVICE
Southeast Regional Office
263 13th Avenue South
St. Petersburg, Florida 33701-5505
(727) 824-5312 FAX 824-5309
<http://sero.nmfs.noaa.gov>

F/SER32:EF

NOV 05 2012

Andreas Fahlman, PhD
Department of Life Sciences
Texas A&M University-Corpus Christi
6300 Ocean Drive, Unit 5892
Corpus Christi, TX 78412

Dear Dr. Fahlman:

The National Marine Fisheries Service (NMFS) has reviewed your request for authorization to receive respiratory system tissues, including trachea, bronchi, and lungs, collected under permit #17530 from bowhead whales (*Balaena mysticetus*). These samples will be used to investigate pulmonary mechanics and biochemical adaptations used for diving. The information provided about your research in your written correspondence is sufficient to satisfy the Marine Mammal Protection Act (MMPA) requirements for transfer of marine mammal parts. The MMPA's implementing regulations at 50 CFR 216.37 (enclosed) authorize the transfer of marine mammal parts if:

- (1) The person/agency transferring the part does not receive payment for the part;
- (2) the marine mammal part is transferred for scientific research purposes, curation in a professionally accredited scientific collection, or educational objectives; and
- (3) an accession number, authorized or assigned by NMFS, is affixed to the marine mammal part. In most cases, this is the field number assigned by the Marine Mammal Stranding Network.

Pursuant to 50 CFR 216.37, this letter authorizes you to receive respiratory system tissues, including trachea, bronchi, and lungs, collected under permit from no more than 15 bowhead whales. **This authorization is valid through October 30, 2016.** Upon expiration, if you would still like to obtain marine mammal parts, please contact Erin Fougères for a renewal of the authorization.

Please note that this parts authorization letter does not guarantee receipt of requested samples. Transfer of parts must be coordinated with the permit holder to ensure that no sample is taken prematurely and to ensure accurate disposition of the parts. Although payment is not allowed for marine mammal parts, the permit holder may assess processing and/or shipping fees. Should you acquire more samples than needed for your scientific research, you must contact the providing permit holder to determine whether the samples should be returned for scientific study or destroyed. Notice of that determination must also be given to this office.

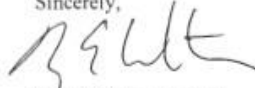


Your acceptance of these marine mammal tissues absolves NMFS and the permit holder of liability for any human health or safety risks, known or unknown, from exposure to these parts.

You are required to provide a written annual report of all specimens received to Erin Fougères, NMFS Southeast Region Stranding Program Administrator, 263 13th Ave South, St. Petersburg FL, 33701. The report should include the specimen/sample type, species, the field identification number of the animal from which the specimen was collected, the animal's original collection date, the date you received the specimen, the organization/individual from which you received the specimen, the final disposition of the specimen (destroyed vs. archived), and the date of the final disposition. The report is due by **February 1, 2013**, and every year thereafter until the expiration of this authorization.

The NMFS Southeast Region requires that you acknowledge the permit holder and NMFS in any publications or other reports resulting from the use of the transferred material or data. Please send copies of these reports to the NMFS Southeast Regional Office for our files and for distribution to the Stranding Network. Reports and questions regarding this authorization should be directed to Erin Fougères at (727) 824-5323 or erin.fougeres@noaa.gov.

Sincerely,



Roy E. Crabtree, Ph.D.
Regional Administrator

Enclosure

cc: F/PR2 – T. Rowles
F/SEC3 – B. Mase-Guthrie
File: 1514-08b.

50 CFR § 216.37 Marine mammal parts.

With respect to marine mammal parts acquired by take or import authorized under a permit issued under this subpart:

(a) Marine mammal parts are transferrable if:

(1) The person transferring the part receives no remuneration of any kind for the marine mammal part;

(2) The person receiving the marine mammal part is:

(i) An employee of NMFS, the U.S. Fish and Wildlife Service, or any other governmental agency with conservation and management responsibilities, who receives the part in the course of their official duties;

(ii) A holder of a special exception permit which authorizes the take, import, or other activity involving the possession of a marine mammal part of the same species as the subject part; or

(iii) In the case of marine mammal parts from a species that is not depleted, endangered or threatened, a person who is authorized under section 112(c) of the MMPA and subpart C of this part to take or import marine mammals or marine mammal parts;

(iv) Any other person specifically authorized by the Regional Director, consistent with the requirements of paragraphs (a)(1) and (a)(3) through (6) of this section.

(3) The marine mammal part is transferred for the purpose of scientific research, maintenance in a properly curated, professionally accredited scientific collection, or education, provided that, for transfers for educational purposes, the recipient is a museum, educational institution or equivalent that will ensure that the part is available to the public as part of an educational program;

(4) A unique number assigned by the permit holder is marked on or affixed to the marine mammal part or container;

(5) The person receiving the marine mammal part agrees that, as a condition of receipt, subsequent transfers may only occur subject to the provisions of paragraph (a) of this section; and

(6) Within 30 days after the transfer, the person transferring the marine mammal part notifies the Regional Director of the transfer, including a description of the part, the person to whom the part was transferred, the purpose of the transfer, certification that the recipient has agreed to comply with the requirements of paragraph (a) of this section for subsequent transfers, and, if applicable, the recipient's permit number.

(b) Marine mammal parts may be loaned to another person for a purpose described in paragraph

(a)(3) of this section and without the agreement and notification required under paragraphs (a)(5) and (6) of this section, if:

(1) A record of the loan is maintained; and

(2) The loan is for not more than one year. Loans for a period greater than 12 months, including loan extensions or renewals, require notification of the Regional Director under paragraph (a)(6).

(c) Unless other disposition is specified in the permit, a holder of a special exception permit may retain marine mammal parts not destroyed or otherwise disposed of during or after a scientific research or enhancement activity, if such marine mammal parts are:

(1) Maintained as part of a properly curated, professionally accredited collection; or

(2) Made available for purposes of scientific research or enhancement at the request of the Office Director.

(d) Marine mammal parts may be exported and subsequently reimported by a permit holder or subsequent authorized recipient, for the purpose of scientific research, maintenance in a properly curated, professionally accredited scientific collection, or education, provided that:

(1) The permit holder or other person receives no remuneration for the marine mammal part;

(2) A unique number assigned by the permit holder is marked on or affixed to the marine mammal specimen or container;

(3) The marine mammal part is exported or reimported in compliance with all applicable domestic and foreign laws;

(4) If exported or reimported for educational purposes, the recipient is a museum, educational institution, or equivalent that will ensure that the part is available to the public as part of an educational program; and

(5) Special reports are submitted within 30 days after both export and reimport as required by the Office Director under § 216.38.

[61 FR 21937, May 10, 1996]

APPENDIX B

Table B1. List of mammalian tracheal samples used in this study. The individual specimens were catalogued with individual characteristics including species, sex, number of tracheal rings, and dimensions of trachea when trimmed of extraneous tissues.

Animal ID	Species	Sex	Tracheal Length (cm)	Tracheal width (cm)	Luminal Width (cm)	Number of Tracheal Rings
DR 001	<i>O. virginianus</i>	male	33.7	2.7	2.4	45.0
DR 002	<i>O. virginianus</i>	male	26.1	2.5	2.3	46.0
DR 003	<i>O. virginianus</i>	male	13.5	2.4	2.2	44.0
KLC 109	<i>T. truncatus</i>	female	13.9	5.6	3.0	13.0
CAHA 066	<i>T. truncatus</i>	female	7.7	2.4	3.2	12.0
CAHA 057	<i>T. truncatus</i>	male	5.7	2.5	2.0	13.0
CAHA 047	<i>T. truncatus</i>	male	10.4	4.3	2.1	12.0
CAHA 038	<i>T. truncatus</i>	male	9.2	3.7	4.5	12.0
MAP 013	<i>T. truncatus</i>	male	14.5	4.4	3.1	12.0
MAP 014	<i>T. truncatus</i>	male	23.2	5.1	4.2	13.0

Table B2. Mean and standard error (SE) for species tracheal dimension values (Table B1).

	Tracheal Length (cm)	Tracheal Width (cm)	Lumen Width (cm)	Tracheal Rings
<i>O. virginianus</i>				
Mean	24.4	2.5	2.3	45
SE	5.8	0.1	0.4	0.6
<i>T. truncatus</i>				
Mean	12.1	4	3.2	12.4
SE	2.2	0.5	0.4	0.2

APPENDIX C

Table C1. All values of elastin coverage for an individual white-tailed deer specimen in this study, along with means, medians and averages for regions, subregions and overall elastin content (D=distal, M=medial, P=proximal, d=dorsal, v=ventral, l=lateral left).

	Dd	Dv	DI	Md	Mv	MI	Pd	Pv	PI
DR001									
<i>O. virginianus</i>	4.8	3.1	4.5	5.8	7.7	6.2	4.3	6.7	7.3
	5.6	4.1	9.3	5.5	11.2	3.6	5.0	8.2	9.7
	6.0	4.5	7.4	6.3	9.0	5.0	8.1	6.6	8.5
	7.8	7.4	5.7	5.9	7.6	7.6	7.3	9.3	9.2
	7.9			7.8	4.8	7.2	7.1		9.4
	8.0					9.8	9.3		
	4.3								
Mean	6.3	4.8	6.7	6.3	8.1	6.6	6.8	7.7	8.8
Median	6.0	4.3	6.6	5.9	7.7	6.7	7.2	7.5	9.2
Overall Mean	6.9								
Overall Median	7.2								
Proximal Mean	7.7								
Medial Mean	6.9								
Distal Mean	6.0								
Dorsal Mean	6.5								
Ventral Mean	6.9								
Lateral Mean	7.4								
Proximal Median	8.1								
Medial Median	6.8								
Distal Median	5.7								
Dorsal Median	6.2								
Ventral Median	7.4								
Lateral Median	7.4								

Table C2. All values of elastin coverage for an individual white-tailed deer specimen in this study, along with means, medians and averages for regions, subregions and overall elastin content (D=distal, M=medial, P=proximal, d=dorsal, v=ventral, l=lateral left).

DR002	Dd	Dv	DI	Md	Mv	MI	Pd	Pv	PI
<i>O. virginianus</i>	7.0	6.7	5.5	5.1	8.0	9.6	7.0	6.7	5.0
	5.4	8.1	7.6	4.3	6.9	8.9	5.7	7.0	5.7
	8.4	7.8	9.9	6.2	8.2	9.0	6.6	8.3	4.5
	9.1	9.6	11.4	7.7	8.3	5.6	5.0		5.9
	4.9	8.5	11.7		8.5	6.0	4.7		6.2
	8.8	10.0	9.2		6.9		7.0		4.3
		10.2	7.3				5.1		
		7.3	6.9						
Mean	7.3	8.5	8.7	5.8	7.8	7.8	5.9	7.3	5.2
Median	7.7	8.3	8.4	5.6	8.1	8.9	5.7	7.0	5.3
Overall Mean	7.3								
Overall Median	7.0								
Proximal Mean	5.9								
Medial Mean	7.3								
Distal Mean	8.2								
Dorsal Mean	6.4								
Ventral Mean	8.1								
Lateral Mean	7.4								
Proximal Median	5.8								
Medial Median	7.7								
Distal Median	8.3								
Dorsal Median	6.2								
Ventral Median	8.1								
Lateral Median	6.9								

Table C3. All values of elastin coverage for an individual white-tailed deer specimen in this study, along with means, medians and averages for regions, subregions and overall elastin content (D=distal, M=medial, P=proximal, d=dorsal, v=ventral, l=lateral left).

DR003	Dd	Dv	Dl	Md	Mv	MI	Pd	Pv	Pl
<i>O. virginianus</i>	10.6	7.9	6.0	4.9	4.8	4.1	7.0	4.8	5.7
	8.9	4.1	5.1	7.9	7.2	4.3	4.7	6.7	5.6
	8.6	7.4	9.7	7.3	7.7	3.8	5.1	5.9	6.2
	9.9	4.8	4.9		8.5	6.3	7.4		6.7
	7.6	6.3	4.7		8.4	5.6	7.9		9.0
	9.1		6.5		12.1	8.9	7.9		
	7.2		8.8		6.7	5.9	5.4		
	7.3		6.9		5.3				
Mean	8.7	6.1	6.6	6.7	7.6	5.6	6.5	5.8	6.7
Median	8.7	6.3	6.3	7.3	7.4	5.6	7.0	5.9	6.2
Overall Mean	6.8								
Overall Median	6.7								
Proximal Mean	6.4								
Medial Mean	6.7								
Distal Mean	7.2								
Dorsal Mean	7.5								
Ventral Mean	6.8								
Lateral Mean	6.2								
Proximal Median	6.2								
Medial Median	6.5								
Distal Median	7.3								
Dorsal Median	7.5								
Ventral Median	6.7								
Lateral Median	5.9								

Table C4. All values of elastin coverage for an individual Atlantic bottlenose dolphin specimen in this study, along with means, medians and averages for regions, subregions and overall elastin content (D=distal, M=medial, P=proximal, d=dorsal, v=ventral, l=lateral left).

CAHA038	Dd	Dv	DI	Md	Mv	MI	Pd	Pv	PI
<i>T. truncatus</i>	8.2	7.5	5.3	9.3	9.4	4.8	9.0	10.1	6.5
	7.3	7.3	7.6	9.7	9.5	5.0	10.2	10.5	14.0
	8.7	5.9	9.1	9.7	8.6	8.8	12.3	11.6	8.5
	8.0	5.6	11.6	8.5	5.6	6.3	14.6	6.8	4.9
	5.7		12.4	8.2	9.8	7.6	7.5	6.0	8.6
	7.5		8.1	11.0	9.3	8.0	6.5	3.9	9.0
	6.9		10.7		7.8	6.6	12.5	7.1	
	9.1		10.3		7.8	4.0	6.7	11.3	
Mean	7.7	6.6	9.4	9.4	8.5	6.4	9.9	8.4	8.6
Median	7.7	6.6	9.7	9.5	8.9	6.4	9.6	8.6	8.6
Overall Mean	8.4								
Overall Median	8.2								
Proximal Mean	9.0								
Medial Mean	8.0								
Distal Mean	8.1								
Dorsal Mean	9.0								
Ventral Mean	8.1								
Lateral Mean	8.1								
Proximal Median	8.8								
Medial Median	8.3								
Distal Median	7.8								
Dorsal Median	8.6								
Ventral Median	7.8								
Lateral Median	8.0								

Table C5. All values of elastin coverage for an individual Atlantic bottlenose dolphin specimen in this study, along with means, medians and averages for regions, subregions and overall elastin content (D=distal, M=medial, P=proximal, d=dorsal, v=ventral, l=lateral left).

CAHA047	Dd	Dv	DI	Md	Mv	MI	Pd	Pv	PI
<i>T. truncatus</i>	6.4	6.5	8.0	14.6	7.2	4.2	7.2	8.2	7.9
	10.3	14.8	10.7	13.5	9.6	11.0	8.0	7.3	10.3
	7.0	12.3	8.9	7.9	7.5	8.0	6.8	7.4	10.8
	8.3		5.7	14.2	11.8		9.3	8.1	9.3
	4.8			9.0	9.8		11.3	7.9	
	6.4			10.5	10.0		10.4	7.3	
	7.9			11.5	10.3			7.6	
	11.2			13.5	8.9				
Mean	7.8	11.2	8.3	11.8	9.4	7.7	8.8	7.7	9.5
Median	7.4	12.3	8.5	12.5	9.7	8.0	8.6	7.6	9.8
Overall Mean	9.2								
Overall Median	8.9								
Proximal Mean	8.5								
Medial Mean	10.2								
Distal Mean	8.6								
Dorsal Mean	9.5								
Ventral Mean	9.0								
Lateral Mean	8.6								
Proximal Median	8.0								
Medial Median	10.0								
Distal Median	8.0								
Dorsal Median	9.2								
Ventral Median	8.1								
Lateral Median	8.9								

Table C6. All values of elastin coverage for an individual Atlantic bottlenose dolphin specimen in this study, along with means, medians and averages for regions, subregions and overall elastin content (D=distal, M=medial, P=proximal, d=dorsal, v=ventral, l=lateral left).

	Dd	Dv	DI	Md	Mv	MI	Pd	Pv	PI
CAHA057									
<i>T. truncatus</i>	11.6	9.1	9.0	10.3	12.6	10.3	10.7	5.0	8.1
	7.4	8.8	6.4	10.9	12.1	10.2	10.4	6.2	9.9
	9.2	9.5	7.4	13.4	12.4	12.3	7.4	5.3	7.4
	7.7	11.1	7.1				7.8	7.4	
	7.1	7.7	6.9				8.4	7.2	
	11.0	8.6	8.8				9.2		
	8.8	8.5	6.2				9.0		
	7.4	8.8	7.2				6.3		
Mean	8.8	9.0	7.4	11.6	12.4	11.0	8.6	6.2	8.5
Median	8.3	8.8	7.1	10.9	12.4	10.3	8.7	6.2	8.1
Overall Mean	8.8								
Overall Median	8.8								
Proximal Mean	7.8								
Medial Mean	11.6								
Distal Mean	8.4								
Dorsal Mean	9.2								
Ventral Mean	8.8								
Lateral Mean	8.4								
Proximal Median	7.6								
Medial Median	12.1								
Distal Median	8.5								
Dorsal Median	9.0								
Ventral Median	8.7								
Lateral Median	7.7								

Table C7. All values of elastin coverage for an individual Atlantic bottlenose dolphin specimen in this study, along with means, medians and averages for regions, subregions and overall elastin content (D=distal, M=medial, P=proximal, d=dorsal, v=ventral, l=lateral left).

CAHA066	Dd	Dv	DI	Md	Mv	MI	Pd	Pv	PI
<i>T. truncatus</i>	10.7	11.6	11.9	9.3	5.0	12.3	7.0	5.7	5.8
	9.0	12.7	12.3	12.5	10.9	10.2	8.0	11.5	7.6
	12.0	11.7	11.3	8.0	8.6	12.1	7.6	7.9	7.0
	6.0	9.5	13.8	12.0	12.8	10.3	7.9	7.1	6.0
	7.2	4.8	13.0	11.5	10.0		6.7		6.2
	11.2			12.8			6.5		8.3
							11.0		9.8
							10.5		
Mean	9.4	10.0	12.5	11.0	9.5	11.3	8.2	8.1	7.2
Median	9.9	11.6	12.3	11.8	10.0	11.2	7.8	7.5	7.0
Overall Mean	9.5								
Overall Median	9.9								
Proximal Mean	7.8								
Medial Mean	10.6								
Distal Mean	10.5								
Dorsal Mean	9.4								
Ventral Mean	9.3								
Lateral Mean	9.9								
Proximal Median	7.6								
Medial Median	10.9								
Distal Median	11.5								
Dorsal Median	9.1								
Ventral Median	9.7								
Lateral Median	10.3								

Table C8. All values of elastin coverage for an individual Atlantic bottlenose dolphin specimen in this study, along with means, medians and averages for regions, subregions and overall elastin content (D=distal, M=medial, P=proximal, d=dorsal, v=ventral, l=lateral left).

KLC109	Dd	Dv	DI	Md	Mv	MI	Pd	Pv	PI
<i>T. truncatus</i>	10.3	12.2	9.2	8.6	8.8	12.0	11.5	8.5	12.9
	9.1	11.7	8.7	9.7	5.6	10.3	12.3	8.9	8.6
	5.4	7.2	11.2	5.7	5.0	10.3	9.4	5.7	11.4
	10.1	7.9	8.7	8.3		9.6		7.1	8.9
	6.4	9.0				8.4		6.0	
	8.1	10.2				7.4			
Mean	8.2	9.7	9.4	8.1	6.5	9.7	11.1	7.3	10.5
Median	8.6	9.6	8.9	8.5	5.6	9.9	11.5	7.1	10.2
Overall Mean	8.9								
Overall Median	8.9								
Proximal Mean	9.3								
Medial Mean	8.4								
Distal Mean	9.1								
Dorsal Mean	8.8								
Ventral Mean	8.1								
Lateral Mean	9.8								
Proximal Median	8.9								
Medial Median	8.6								
Distal Median	9.0								
Dorsal Median	9.1								
Ventral Median	8.2								
Lateral Median	9.4								

Table C9. All values of elastin coverage for an individual Atlantic bottlenose dolphin specimen in this study, along with means, medians and averages for regions, subregions and overall elastin content (D=distal, M=medial, P=proximal, d=dorsal, v=ventral, l=lateral left).

MAP013	Dd	Dv	DI	Md	Mv	MI	Pd	Pv	PI
<i>T. truncatus</i>	12.2	12.9	6.5	5.6	8.5	6.5	8.6	6.6	7.6
	8.9	12.1	9.1	7.4	6.3	7.0	8.0	11.4	9.0
	8.7	15.7	8.2	9.2	5.5	10.2	9.1	8.4	5.2
	16.0	11.7	10.3	9.1	8.1	11.0	6.8	10.1	
	16.2	7.8			6.6		10.8	9.6	
	10.7	9.6			7.8			10.8	
	10.5	9.7						6.7	
		14.3							
Mean	11.9	11.7	8.6	7.8	7.1	8.7	8.7	9.1	7.3
Median	10.7	11.9	8.7	8.2	7.2	8.6	8.6	9.6	7.6
Overall Mean	9.3								
Overall Median	9.0								
Proximal Mean	8.6								
Medial Mean	7.8								
Distal Mean	11.1								
Dorsal Mean	9.9								
Ventral Mean	9.5								
Lateral Mean	8.2								
Proximal Median	8.6								
Medial Median	7.6								
Distal Median	10.5								
Dorsal Median	9.1								
Ventral Median	9.6								
Lateral Median	8.2								

Table C10. All values of elastin coverage for an individual Atlantic bottlenose dolphin specimen in this study, along with means, medians and averages for regions, subregions and overall elastin content (D=distal, M=medial, P=proximal, d=dorsal, v=ventral, l=lateral left).

MAP014	Dd	Dv	DI	Md	Mv	MI	Pd	Pv	PI
<i>T. truncatus</i>	6.1	5.3	14.4	5.3	7.7	8.9	9.4	7.7	11.5
	9.0	4.9	12.4	7.0	10.9	11.1	11.2	8.3	6.1
	6.1	3.3	13.5	4.7	10.8	7.0	11.3	7.4	10.3
	8.1	3.9	13.8	6.1	9.9	8.9	12.1	8.4	6.8
	13.4	8.5	9.4	5.4	9.2	10.8	12.9	5.4	8.4
		4.5	6.8	6.8	7.7	9.5	8.1	3.5	12.5
		5.0	4.8		6.1	3.7	6.4		11.0
		7.8	5.8		9.1	4.1	6.2		5.5
Mean	8.5	5.4	10.1	5.9	8.9	8.0	9.7	6.8	9.0
Median	8.1	5.0	10.9	5.7	9.2	8.9	10.3	7.5	9.4
Overall Mean	8.1								
Overall Median	7.8								
Proximal Mean	8.7								
Medial Mean	7.8								
Distal Mean	7.9								
Dorsal Mean	8.2								
Ventral Mean	7.1								
Lateral Mean	9.0								
Proximal Median	8.3								
Medial Median	7.7								
Distal Median	6.8								
Dorsal Median	7.0								
Ventral Median	7.7								
Lateral Median	9.2								

APPENDIX D

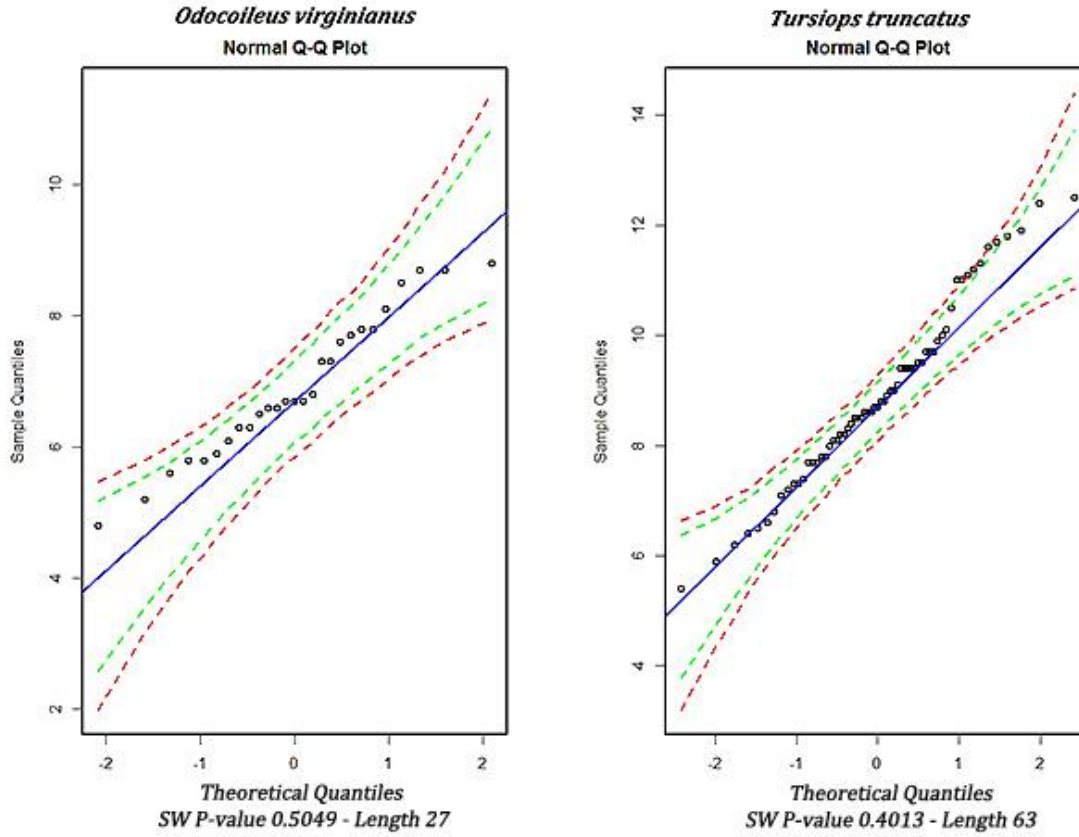


Figure D1. Data points for individual species population means in Q-Q plots. The data points presented against predicted residual regression line (blue) with simulated boundaries indicating one (green) and two (red) standard deviations. Shapiro-Wilk values were calculated as a secondary, quantitative evaluation of population normality ($\alpha = 0.05$).

APPENDIX E

Table E1. Analysis of variance (ANOVA) for intraspecies variation of elastin abundance of the two examined species. Degrees of freedom (df) were commensurate with sample size for three *Odocoileus virginianus* and seven *Tursiops truncatus* specimens.

ANOVA		df	F value	P-value
Intraspecies				
<i>O. virginianus</i>				
	Region	2	0.183	0.835
	Subregion	2	0.247	0.783
	Region*Subregion	4	1.008	0.429
	(Within)	18		
<i>T. truncatus</i>				
	Region	2	0.809	0.450
	Subregion	2	0.807	0.451
	Region*Subregion	4	0.591	0.671
	(Within)	54		

Table E2. Mean values for species (in %) calculated for an overall value; as well as each region and subregion.

Species	Proximal	Medial	Distal	Dorsal	Lateral	Ventral
<i>T. truncatus</i>	8.7	9.4	9.3	9.4	9.3	8.7
<i>O. virginianus</i>	6.9	6.8	7.1	6.6	7.0	7.2

APPENDIX F

***Tursiops truncatus trachea* (ventral view)**

(Rotated left along sagittal plane)

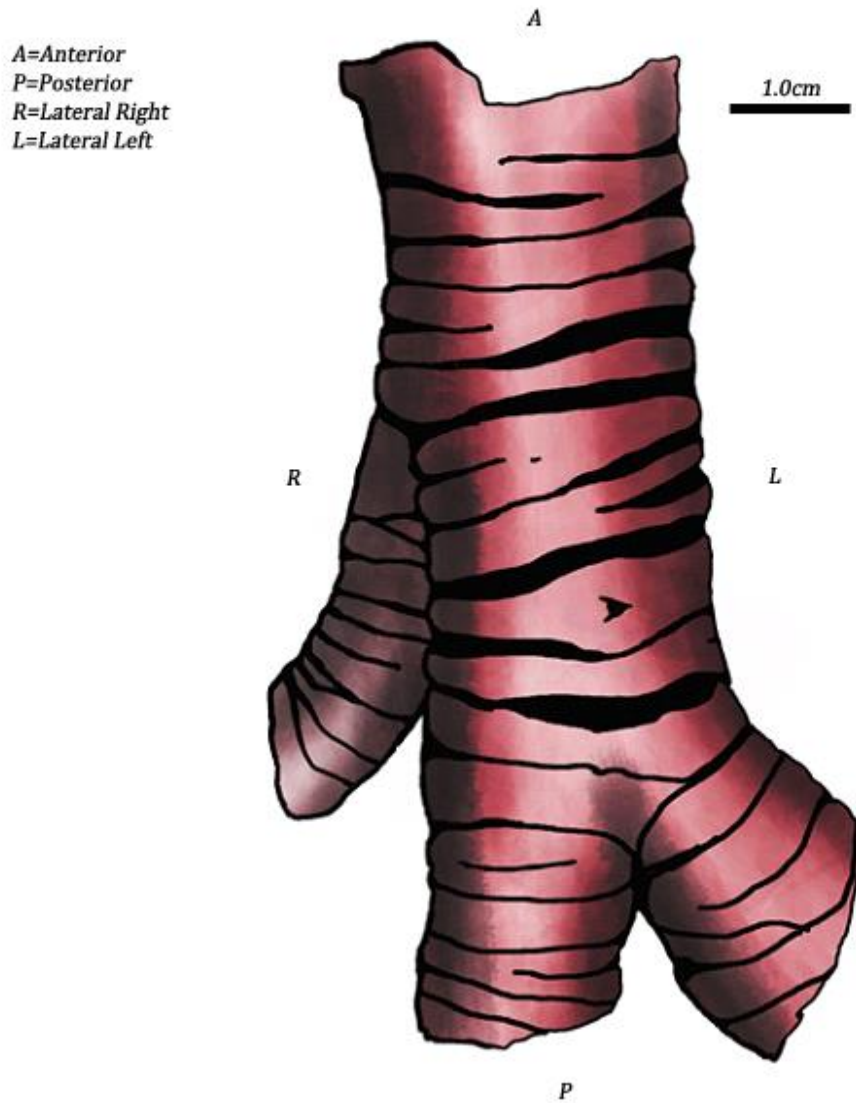


Figure F1. Illustration of an Atlantic bottlenose dolphin trachea (Ventral view) with anastomosing cartilaginous rings (A-anterior, P-posterior, R-right, L-left).



Figure F2. Illustration of an Atlantic bottlenose dolphin (*Tursiops truncatus*) trachea (Ventral Left view) with anastomosing cartilaginous rings (A-anterior, P-posterior).

(lateral left view)



Figure F3. Illustration of an Atlantic bottlenose dolphin trachea (Lateral Left view) with anastomosing cartilaginous rings (A-anterior, P-posterior, L-left).

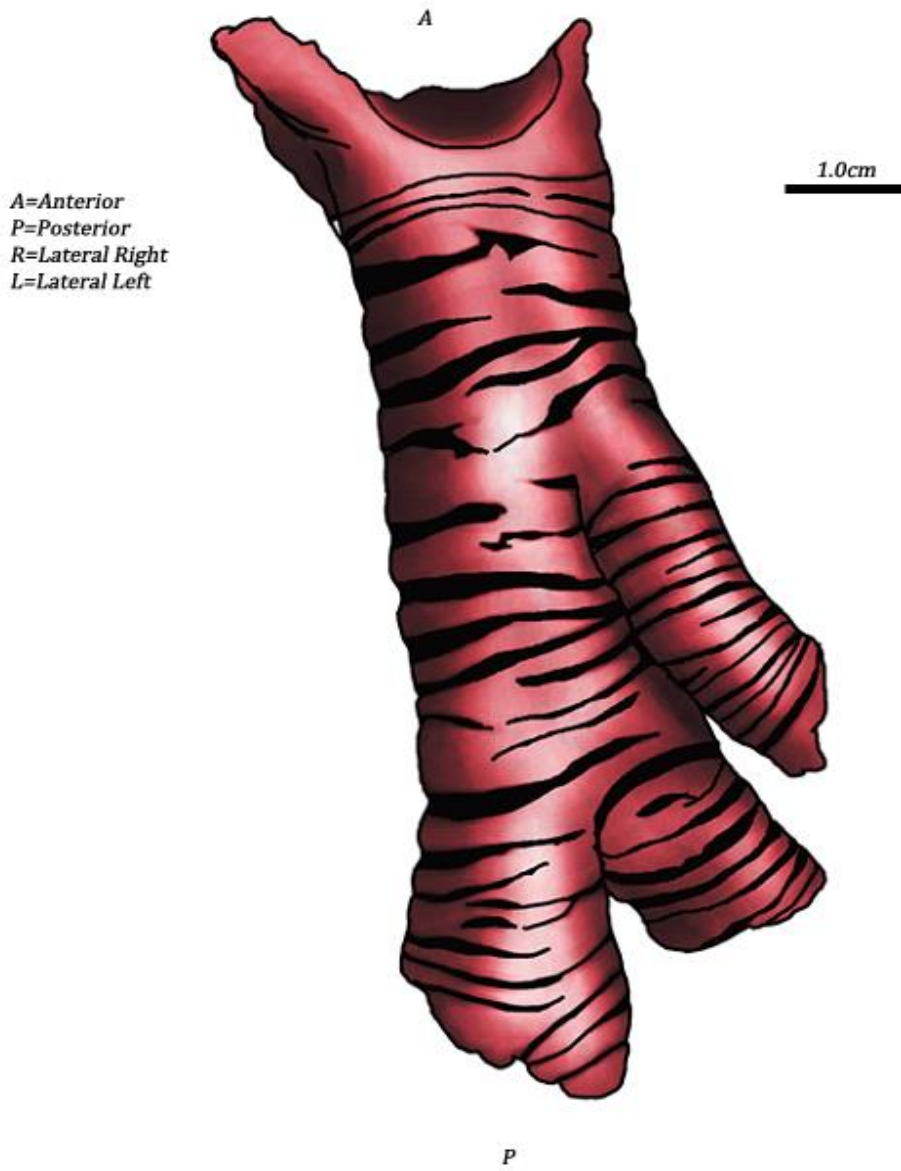


Figure F4. Illustration of an Atlantic bottlenose dolphin trachea (Dorsal Left view) with anastomosing cartilaginous rings (A-anterior, P-posterior).

(dorsal view)

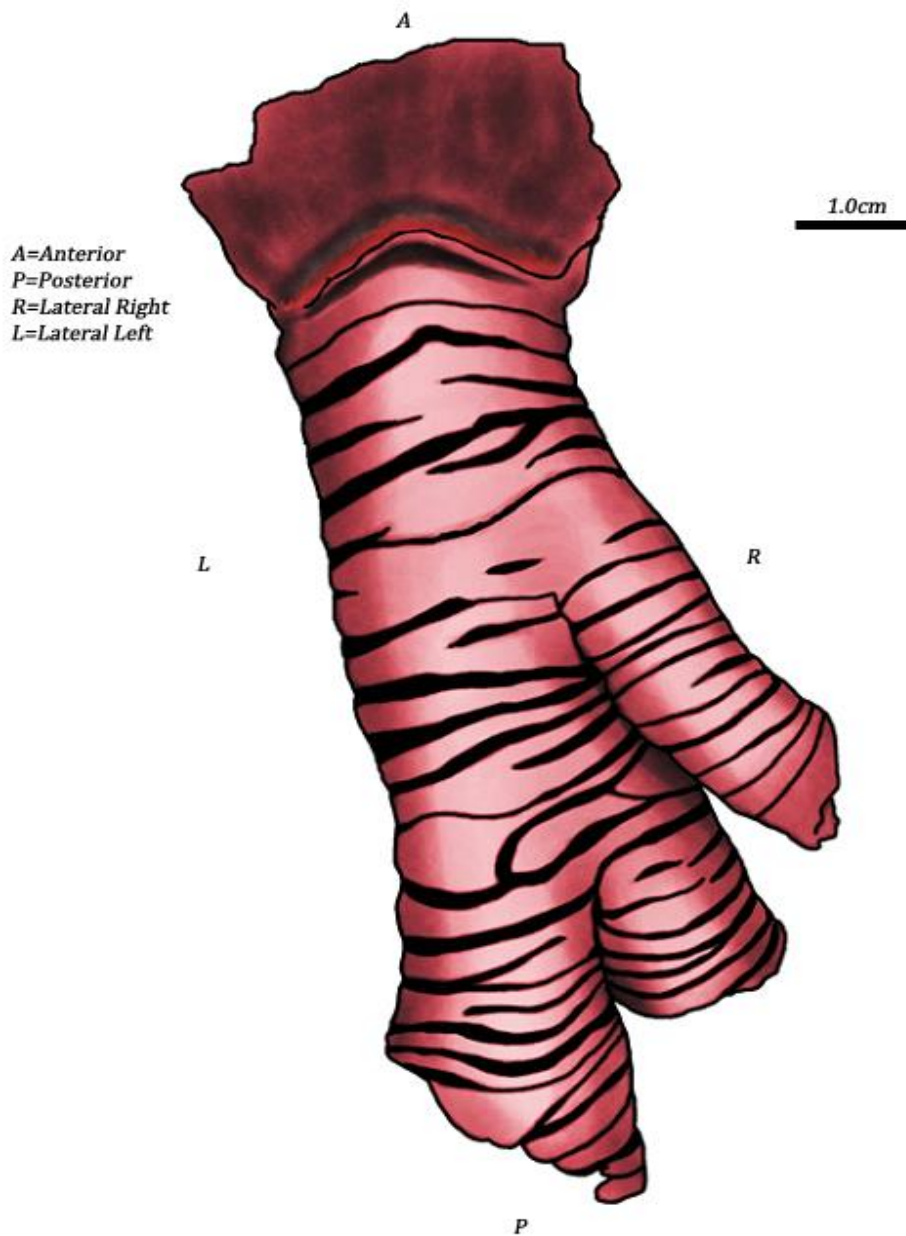


Figure F5. Illustration of an Atlantic bottlenose dolphin trachea (Dorsal view) with anastomosing cartilaginous rings (A-anterior, P-posterior, R-right, L-left).

APPENDIX G

Tursiops truncatus

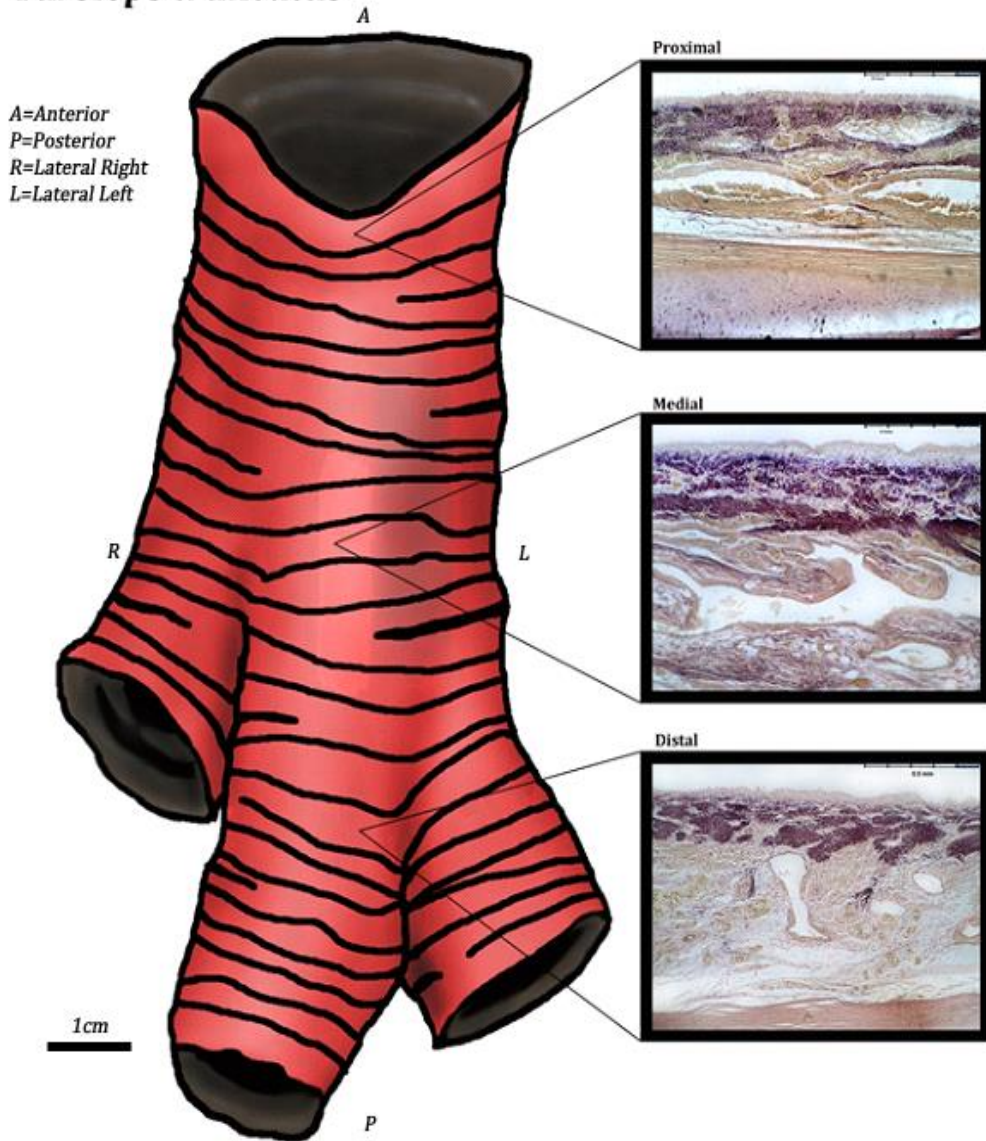


Figure G1. Ventral view of Atlantic bottlenose dolphin trachea showing regional distribution of tracheal elastin (A=anterior, P=posterior, R=right, L=left).

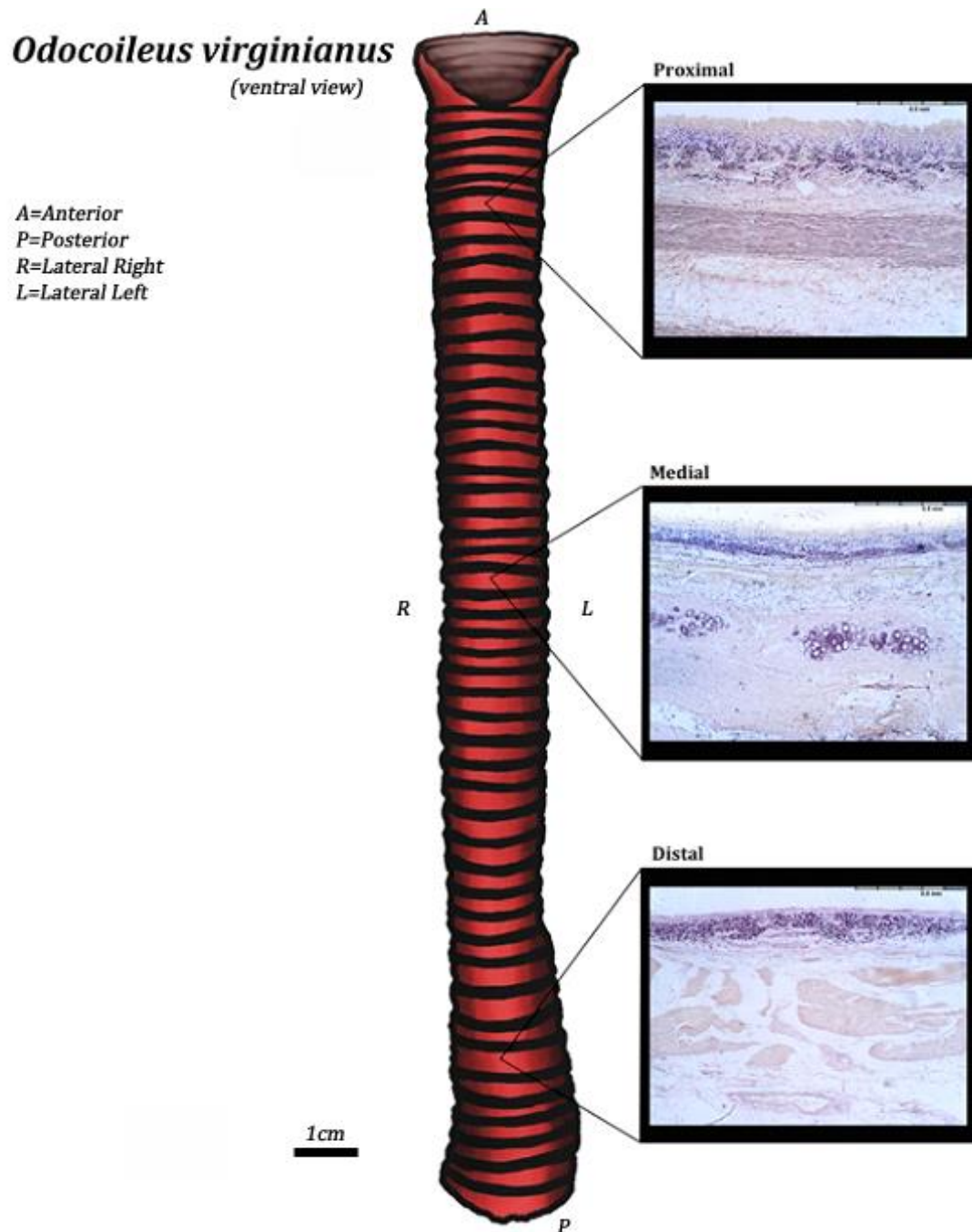


Figure G2. Ventral view of white-tailed deer trachea showing regional distribution of tracheal elastin (A=anterior, P=posterior, R=right, L=left).